EFFECTS OF CALCITONIN GENE DELETION ON FETAL-PLACENTAL CALCIUM METABOLISM AND MATERNAL FERTILITY

KIRSTEN RAE McDONALD

INFORMATION TO USERS

This manuscript has been reproduced from the microfilm master. UMI films the text directly from the original or copy submitted. Thus, some thesis and dissertation copies are in typewriter face, while others may be from any type of computer printer.

The quality of this reproduction is dependent upon the quality of the copy submitted. Broken or indistinct print, colored or poor quality illustrations and photographs, print bleedthrough, substandard margins, and improper alignment can adversely affect reproduction.

In the unlikely event that the author did not send UMI a complete manuscript and there are missing pages, these will be noted. Also, if unauthorized copyright material had to be removed, a note will indicate the deletion.

Oversize materials (e.g., maps, drawings, charts) are reproduced by sectioning the original, beginning at the upper left-hand corner and continuing from left to right in equal sections with small overlaps.

ProQuest Information and Learning
300 North Zeeb Road, Ann Arbor, MI 48106-1346 USA
800-521-0600

EFFECTS OF CALCITONIN GENE DELETION ON FETAL-PLACENTAL CALCIUM METABOLISM AND MATERNAL FERTILITY

by

© Kirsten Rae M'Donald

A thesis submitted to the

School of Graduate Studies

in partial fulfillment of the

requirements for the degree of

Master of Science

Department of Basic Medical Sciences
Faculty of Medicine
Memorial University of Newfoundland

December, 2001

St. John's Newfoundland

ABSTRACT

Very little is known about how calcium metabolism is regulated in the fetus, and in particular, the role of calcitonin (CT) has not been established. We studied fetal mice in which the CT gene has been deleted to determine whether CT is critically required for normal fetal-placental calcium homeostasis and skeletal development.

We demonstrated that homozygous deletion of the CT gene eliminated CT but did not affect maternal or fetal ionized calcium levels, the rate of fetal-placental calcium transfer, serum phosphorus levels, or the amount of mineral present in each fetal skeleton. It also did not affect the gross skeletal morphology, the expression of important bone markers, fetal serum parathyroid hormone (PTH) levels, or calbindin-D_{9K} or Ca^{++} ATPase expression in placental tissue. However, maternal loss of CT resulted in a reduction in litter size while both maternal and fetal loss of CT resulted in a reduction in the concentration of magnesium in the fetal circulation and possibly in the fetal skeleton. Our studies also confirm that the genes for CT and the CT-receptor are located in the murine placenta.

In summary, these results suggest that CT cannot cross the placenta, that the maternal absence of CT reduces the total number of fetuses that survive at term, and that CT may selectively regulate aspects of magnesium metabolism in the fetus. However, it appears that the complete loss of either maternal or fetal CT does not perturb the other measured parameters of fetal-placental calcium homeostasis.

ACKNOWLEDGEMENTS

My sincere thanks to Dr. Christopher Kovacs for the guidance, advice and supervision he has given me throughout my program. Many thanks to the members of my supervisory committee, Dr. Gary Paterno and Dr. George Carayanniotis, for providing helpful comments and expertise.

I would like to acknowledge the creators of the CT-knockout mice, Dr. Ana Hoff, Dr. Gilbert Cote, and Dr. Robert Gagel, as well as Dr. James Friel, Claude Mercer, and Judy Foote for their technical assistance. Special thanks to Dr. Alan Pater, Dr. Shou-Ching Tang, and Gary Chernenko for providing me with the use of their equipment and facilities. I would also like to acknowledge the Department of Research and Graduate Studies, Faculty of Medicine, for their financial assistance.

I would especially like to recognize Linda Chafe, Neva Fudge, and Mandy Woodland for their helpful assistance, friendship, and for making our lab such a happy place. Special thanks to my wonderful friends Adam, Beth, Jason, and all of my fellow graduate students here at MUN that have made the past 2 years so enjoyable.

Most importantly, I can never express enough appreciation to my family, Mom, Dad, and Murray, as well as my best friends, Gordon, Erin, Gina, and Deanna for their unconditional love, encouragement, and support.

TABLE OF CONTENTS

LIST OF TABLES

LIST OF FIGURES

LIST OF ABBREVIATIONS

ANOVA	Analysis of Variance
bp	Base Pairs
Ca^{++}	Ionized Calcium
Ca^{2+}ATPase	Calcium Pump
CGRP	Calcitonin Gene-Related Peptide
CMP	Cartilage Matrix Protein
CT	Calcitonin
DAB	3,3'-diaminobenzidine
DNA	Deoxyribonucleic Acid
DTT	Dithiothreitol
EDTA	Ethylene Diamine Tetra Acetic Acid
ELISA	Enzyme-Linked ImmunoSorbent Assay
EPYS	Extraplacental Yolk Sac
HCL	Hydrochloric Acid
HET	Heterozygote
HOM	Homozygote
IPYS	Intraplacental Yolk Sac
IRMA	Immunoradiometric Assay
KOH	Potassium Hydroxide
mRNA	Messenger Ribonucleic Acid

n	Number of Observations
NaCl	Sodium Chloride
NEO	Neomycin
NS	Non-significant
P	Probability
PBS	Phosphate Buffered Saline
PCR	Polymerase Chain Reaction
PTH	Parathyroid Hormone
PTHrP	Parathyroid Hormone-Related Protein
RNA	Ribonucleic Acid
RT-PCR	Reverse Transcriptase Polymerase Chain Reaction
SDS	Sodium Dodecyl Sulfate
SE	Standard Error
TAE	Tris Acetic Acid-EDTA
TEA	Triethanolamine
WT	Wild-type

I. INTRODUCTION

1.1 Calcium and Bone Homeostasis

Normal calcium and bone homeostasis is the process by which humans and other mammals maintain the calcium concentration in blood at a critical and tightly controlled level for normal cellular functioning as well as maintain a sturdy, fully mineralized skeleton. Calcium plays a key role in cellular physiology and metabolic regulation in all organisms. In humans specifically, extracellular calcium levels are tightly regulated within a narrow range so that many tissues can function properly. The intracellular calcium levels are also tightly controlled, at levels approximately 10,000-fold lower than extracellular calcium, so that calcium can serve as an intracellular second messenger (1).

About 99% percent of the total calcium in the human body is present in bone. 99% percent of this bone calcium is located within the crystalline structure of the mineral phase. The remaining 1% is rapidly exchangeable with the extracellular calcium pool. Extracellular calcium acts as the principal substrate for the mineralization of cartilage and bone (2). In bone, calcium salts provide the structural integrity of the skeleton, while in the extracellular fluids and cytosol, the ionized calcium concentration [Ca^{++}] is important in maintaining and controlling biochemical processes (3). Ionized calcium makes up about 50% of the total calcium in serum and extracellular fluids whereas 40% is protein bound and 10% is complexed with phosphate and citrate (1).

Phosphorus and magnesium are also important components of bone. About 15% of the phosphorus in the human body is present in the extracellular fluids whereas 85%

plays a structural role in crystalline form in the skeleton (3). About two thirds of the magnesium present in the adult human body is present in the skeleton while the remaining one third is present in soft tissues. The magnesium in bone appears to be located on the crystalline structure (3).

In the adult, calcium and bone homeostasis is maintained by the interactions of hormones including parathyroid hormone (PTH), calcitriol, and possibly calcitonin (CT). **PTH** is a peptide hormone that controls the level of ionized calcium present in the blood and extracellular fluids. In response to an increase in blood calcium, the parathyroid gland decreases its synthesis and secretion of PTH (2). The main function of PTH is to increase blood calcium and it achieves this by binding to cell surface receptors predominantly in bone and kidney. In bone, PTH stimulates the release of calcium and phosphate, while in the kidney it stimulates reabsorption of calcium and inhibits the reabsorption of phosphate (3). **Calcitriol** also helps keep the level of calcium in serum within normal range. This steroid hormone acts primarily by increasing intestinal absorption of calcium from the diet but also has functions in kidney and bone that are relevant to calcium homeostasis. Calcitriol has functions in other tissues as well, including the recruitment of stem cells in the bone to become mature osteoclasts, which release calcium stores from the bone into the circulation. Serum calcium levels tightly regulate the renal production of calcitriol through the actions of PTH and phosphorus (4). **CT** is known to regulate blood calcium in lower vertebrates, such as fish, but the role of CT and its importance in human calcium homeostasis is less certain (see section 1.3).

1.2 Calcium and Bone Homeostasis in the Fetus

Little is known about how fetal calcium and bone homeostasis is regulated. The fetus must adapt itself in such a way so as to meet its special needs during development. These special needs are that 1) the fetus must ensure that it receives enough calcium to fully mineralize its skeleton by the time of birth and 2) at the same time, the fetus faces the challenge of maintaining a calcium concentration in the blood that is higher than the normal adult (and maternal) level (5). In order to achieve these goals, the fetus must make use of the placenta, kidneys, bone and intestine (reviewed in (6)).

The known calciotropic hormones and other possible (as yet unknown) factors are responsible for regulating blood calcium and directing calcium into the skeleton as it develops. Evidence suggests that both PTH and PTH-related protein (PTHrP) are required for normal regulation of fetal blood calcium through their actions on fetal bone and kidneys (5). However, PTH has been shown to have a greater impact on blood calcium regulation than PTHrP (7) (8). That is, loss of PTH causes a greater lowering of the blood calcium than loss of PTHrP, while loss of both PTH and PTHrP results in the lowest blood calcium level. It is possible that other factors such as CT, calcitriol, and the sex steroids are involved, but such findings have yet to be reported.

The fetus must meet the demands of the mineralizing skeleton by actively transporting calcium across the placenta; the rate of passive or diffusional flow across the placenta is too slow compared to the daily calcium accretion rate by the skeleton late in gestation. The roles of PTH, PTHrP, calcitriol, and CT in regulation of placental calcium transfer have been studied to varying degrees. Evidence suggests that PTHrP is an

important regulator of placental calcium transfer while PTH appears to have no effect (9). The roles of calcitriol, CT, and the sex steroids remain uncertain (reviewed in (6)).

It is known that the fetus maintains a higher blood calcium (both total and ionized) than the circulating maternal level and the fetus establishes its particular blood calcium level independently of the circulating maternal blood calcium level (10). The physiological significance of this fetal hypercalcemia has not been determined (reviewed in (6)).

The fetal kidneys may play a role in regulating the fetal blood calcium level by adjusting the relative reabsorption and excretion of calcium and phosphate. However, there is little data available on fetal kidney function and its relative importance in regulating the fetal blood calcium. Renal excretion of calcium (and other minerals) does not necessarily imply that the fetus will experience a permanent loss of calcium since the urine becomes part of the amniotic fluid which can be swallowed and the calcium made available again to the fetus. Measurements of the volume and composition of amniotic fluid are often used as indirect measures of fetal renal function (reviewed in (6)) but are confounded by the fact that other tissues (such as lungs, placenta, and uterine decidua) may contribute to the composition of the amniotic fluid.

The fetal skeleton also appears to play an important role in fetal calcium homeostasis. This is expected since as the skeleton grows and mineralizes, most of the calcium is present in bone. Evidence suggests that the calcium present in the bone can be mobilized in response to a reduction in the transfer of calcium from the mother to the fetus. For example, when fetuses are hyperparathyroid, with an even higher blood

calcium than normal, the skeleton becomes under-mineralized to help maintain that increased blood calcium level (10). Thus, an exchange between bone calcium and blood calcium is most likely occurring in order to maintain the ionized calcium concentration in the blood. In addition, it is known that normal mineralization of the fetal skeleton requires intact parathyroid glands as well as adequate delivery of calcium to the fetal circulation (reviewed in (6)). In the presence of a low blood calcium level, such as in fetal mice that lack PTH, the skeleton organifies normally but is significantly under-mineralized (8).

1.3 Calcitonin

CT is a peptide hormone which functions to regulate blood calcium in fish. However, the physiological role of CT in human calcium and skeletal metabolism has not yet been established. A Canadian scientist, D. Harold Copp, discovered the hormone in 1961 during perfusion studies of the thyroid and parathyroid glands of dogs. Copp had discovered a hormone which was released by hypercalcemia and acted to lower the plasma calcium. He decided to name the hormone "calcitonin" since it appeared to be involved in regulating the level or "tone" of calcium in the body fluids (11). Copp had thought that the hormone originated in the parathyroid glands, however it was later confirmed that CT originated in the thyroid gland (12). More specifically, CT is produced in parafollicular cells of the thyroid, called C cells, referring to their responsibility for CT secretion (13). The C cells arise from the neural crest and migrate

forward to become the ultimobranchial body in lower vertebrates or the parafollicular cells in humans and related species (14).

CT is a 32-amino-acid polypeptide that contains a disulfide bridge between the cysteine residues in positions 1 and 7, forming a seven membered ring at the N terminal (15). All CT species have the same basic structure but have been classified into three main groups. These groups are (1) artiodactyl (porcine, ovine, and bovine), (2) human and rat, and (3) teleost (salmon, eel, and chicken) (16). The human CT gene contains six exons and is located on the short arm of chromosome 11 (2). Differential splicing of the exon regions in the initial gene transcript produces two distinct mature messenger RNAs. One translates as a 141-residue CT precursor while the other translates as a 128-residue precursor for calcitonin gene-related peptide (CGRP). CT is the major posttranslational product of C cells, whereas CGRP (a 37-amino-acid peptide) is the major posttranslational product in neurons (17).

CT carries out its biologic effects through the CT-receptor which is a G protein-coupled cell surface receptor that is closely related to the receptor for PTH. The CT-receptor is robustly expressed in osteoclasts as well as in the kidney and certain areas of the brain (17). Several isoforms of the CT-receptor have been described, however the functional significance of this is not known. The receptor is widely expressed and also binds CGRP (2).

Several organ systems are involved in the metabolism of CT. Evidence suggests that the hormone may be degraded by the kidneys, liver, bone, and even the thyroid gland. However in most studies, the kidney appears to be the important organ for

clearance of CT (17). CT disappears from plasma in a multi-exponential manner whereby the half-life of the peptide in blood is only a few minutes (18).

The primary biologic effect of CT is to inhibit osteoclastic bone resorption. It accomplishes this by causing the osteoclast to shrink and decrease its bone-resorbing activity and this process is mediated by the CT-receptor. When bone turnover is sufficiently high, CT will produce hypocalcemia and hypophosphatemia. Controversial reports have also suggested that CT might inhibit osteocytes and stimulate osteoblasts (17). In addition, the presence of CT and its receptor at intracranial sites may qualify CT as a neurotransmitter (17).

CT is secreted by several endocrine malignancies and therefore can serve as a tumor marker for diseases such as medullary thyroid carcinoma. Also, CT levels may be elevated in severely ill patients, such as those with burn inhalation injury, toxic shock syndrome, and pancreatitis (2). Because CT inhibits osteoclastic bone resorption, the hormone is commonly used as a therapeutic agent. It is used to treat disorders associated with excess bone resorption, such as osteoporosis and Paget's disease. Analgesia is a commonly reported effect of CT treatment of patients with vertebral crush fractures, osteolytic metastases, or phantom limb (2). CT has also been reported to act as an antiinflammatory agent, to promote fracture and wound healing, to increase the excretion of uric acid, to be antihypertensive, and to impair glucose tolerance (17).

It was thought for many years that as a hypocalcemic hormone, CT might be important in controlling plasma calcium. For example, evidence from work with young pigs suggests that, in the short term (1-2 hours), the loss of CT leads to a small but

significant increase in plasma calcium concentration that can be restored to normal by infusion of porcine CT at the basal rate of secretion (19), and also that CT may be important in maintaining the plasma calcium concentration within normal limits following a meal (20). However, evidence in humans now suggests that CT may not be required. The levels of CT in the circulation decrease in response to hypocalcemia and likewise increase in response to hypercalcemia, yet it is uncertain that these changes in *physiological* levels of CT have an important biological effect. When CT is presented at levels up to 10,000 fold higher than normal, as in those with medullary thyroid carcinoma, there is no detectable abnormality of calcium or bone homeostasis. Conversely, the absence of CT as a result of thyroid resection for thyroid cancer, does not impair calcium or bone homeostasis. Finally, it is important to note that many of the actions attributed to CT have been observed as a result of *pharmacological* doses of the hormone, doses that far exceed the normal *physiological* concentrations of the hormone. While CT has been shown to be important for calcium homeostasis in lower organisms (such as the fishes), it is possible that the hormone has become vestigial or obsolete in humans and other mammals. Nonetheless, it is still possible that CT plays a role in normal calcium homeostasis by protecting the body's calcium stores during times of calcium stress, such as during pregnancy and lactation, growth, and aging (16). For example, increased levels of CT might help protect the maternal skeleton against excessive demineralization during pregnancy and lactation (see section 1.4).

CGRP, a 37-amino-acid peptide, is the major processed peptide in neurons and thus functions as a neurotransmitter. CGRP is known to be a potent vasodilator that

might play an important role in cardiovascular regulation (16). CGRP reacts with the CT-receptor and like CT, the relevance of CGRP to skeletal metabolism is unknown. It may be produced locally in the skeletal tissue and exert a local regulatory effect (17). Since bone is highly vascularized and innervated, it is also quite possible that CGRP plays a role in normal skeletal physiology.

1.4 Calcitonin's Role in Pregnancy and Lactation

In human pregnancy, serum CT levels have generally been reported to be higher than nonpregnant levels and the thyroidal C cells, breast, and placenta have been found to be sites of CT synthesis during pregnancy (reviewed in (6)). One postulated role of CT is that it might protect the maternal skeleton from severe calcium resorption during pregnancy and lactation. However, an adequate experimental model of CT deficiency had not previously been created, partly due to the fact that extrathyroidal sites of CT synthesis were not appreciated at the time (reviewed in (6)). For example, in 1975, a study was done using thyroidectomized rats whose parathyroids had been removed and transplanted to the thigh muscle, and who were injected with thyroxine to restore the animals to a euthyroid but CT-deficient condition. If was found that the thyroidectomized rats had lower bone, total ash, and total calcium weights than control animals 24 days after parturition (21). The results of this study suggest that CT protects the skeleton from excessive resorption that would otherwise occur in thyroidectomized rats during pregnancy, since in the absence of CT, the skeleton lost mineral. However, the results of this study are suspect since thyroid hormone levels and CT levels were not measured

following thyroidectomy to ensure that a euthyroid condition had been attained. In another study, goats were thyroparathyroidectomized, with the parathyroids auto-transplanted elsewhere in the animal, and were injected with thyroxine to create an apparently normocalcemic, euthyroid but CT-deficient animal. When fed a calcium deficient diet, these goats lost more bone mineral by day 60 of lactation than control (sham-operated) animals (22) (23). However, this model still suffers from the fact that thyroxine, thyroid stimulatory hormone, ionized calcium, PTH, and CT levels were not measured to confirm that the model truly was what it was designed to be. It has not been technically feasible to determine whether this postulated role of CT is operative during human pregnancy.

1.5 Calcitonin's Role in Fetal-Placental Calcium and Bone Homeostasis

As with adult calcium physiology, the exact role (if any) of CT in fetal calcium homeostasis and skeletal metabolism remains to be established. It has been found, by radioimmunoassay, that immunoreactive CT can be detected in human fetal thyroid glands as early as week 15 of gestation (24), and that fetal CT levels are maintained at higher levels than maternal (25) (reviewed in (6)). The increased levels of CT in the fetus may reflect increased synthesis, however the metabolism and clearance of CT have not yet been studied in fetal animals. In addition, evidence in rats suggests that maternal CT is not able to cross the placenta (26).

Several studies suggest that CT might play a role in fetal calcium homeostasis. For example, one study demonstrated that infusing CT antiserum to fetal rats increased

blood calcium in the fetus after 1 hour (27). In a study on thyroidectomized sheep which were injected with ^{45}Ca, the amount of ^{45}Ca accumulation in fetal skeletons (during week 19 of gestation) was significantly greater in fetuses of sheep that were supplemented with thyroxine alone than in those supplemented with thyroxine and CT or in control animals (28). In a similar study on intact fetal sheep, CT was found to reduce PTHrP-mediated increases in calcium accumulation in the fetal skeleton but CT alone had no significant effect upon transplacental flux of calcium as measured by the accumulation of ^{45}Ca in the fetal skeleton after administration of ^{45}Ca to the mother (29). It was later demonstrated in sheep that fetal thyroidectomy combined with replacement of thyroxine had no effect on blood calcium in the fetus (30). Taken together, these studies suggest that CT is not involved in fetal calcium homeostasis.

1.6 The Growth Plate

The development of fetal bone is a process which is intimately involved in calcium metabolism and is very sensitive to disruptions in calcium and bone homeostasis. In mammals, bone development occurs by a process known as endochondral ossification which occurs at the growth plate, a specialized tissue that is located at the distal and proximal ends of long bones (Figure 1). The role that CT normally plays in the process of fetal bone development has not yet been determined.

The growth plate controls the extension of long bones through a complex sequence of events, which has been described in detail (31). Following mesenchymal cell condensation, the process begins with the formation of a cartilaginous scaffold that is

Figure 1. Endochondral ossification in the mammalian growth plate. The regions of the growth plate include the zone of resting cartilage, zones of proliferation and maturation, and a zone of hypertrophic cell cartilage. Blood vessels invade the hypertrophic area and osteoclasts resorb the ossified cartilaginous matrix. Osteoblasts derived from the bone collar replace this matrix with bone. (Adapted from (31))

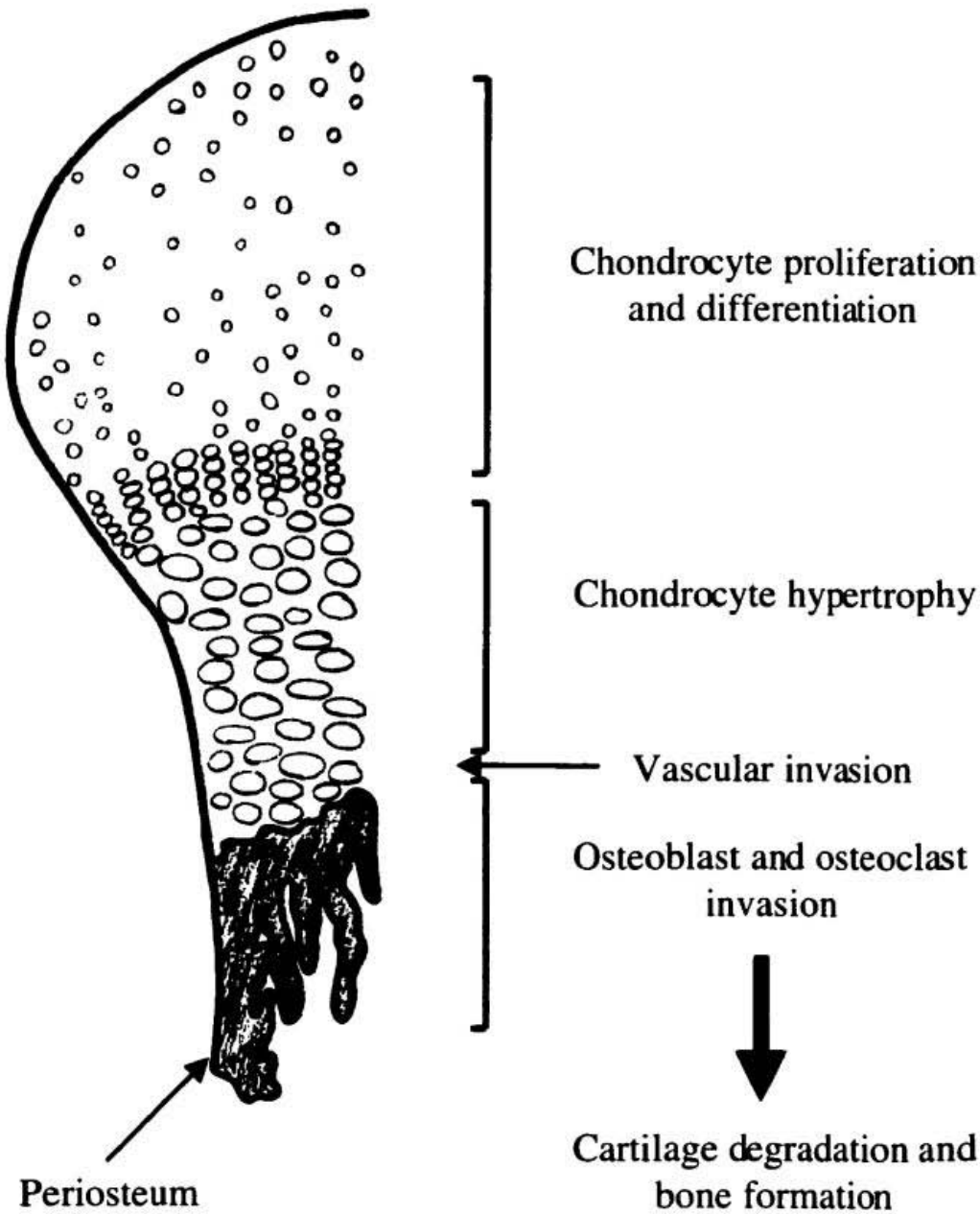
Chondrocyte proliferation and differentiation
Chondrocyte hypertrophy
Vascular invasion
Osteoblast and osteoclast invasion
Cartilage degradation and bone formation
Periosteum

later replaced by bone matrix. The mesenchymal cells then differentiate into collagen producing cells which proliferate until the shape of the future bone is established. The cells located at the centre of this structure further differentiate into hypertrophic chondrocytes. These cells are responsible for synthesizing a cartilaginous matrix that eventually calcifies. Simultaneously, mature hypertrophic chondrocytes undergo apoptosis, allowing blood vessels to invade the region, and a combination of multinucleate, matrix resorbing cells, and differentiated osteoblasts appear. The cartilaginous matrix is then degraded and is replaced by an osteoblast secreted bone matrix. This organic matrix later accretes mineral and becomes calcified, mature bone. The only cartilaginous structures which remain when the process is complete are the growth plate cartilages located at the two distal ends of the bone (31).

Although the terminology used to describe the various zones of chondrocytes in the growth plate varies greatly, it is generally accepted that there are four main regions present. These include a zone of resting cartilage, a zone of proliferating chondrocytes, a zone of differentiating chondrocytes, and a zone of hypertrophic chondrocytes.

1.7 The Placenta

The fetus and placenta must acquire enough calcium to allow the fetal skeleton to mineralize and to ensure that the extracellular calcium level is physiologically suitable for fetal tissues (5). It is possible that maternal hormones influence the transport of calcium across the placenta by affecting the level of maternal calcium in circulation as well as by

directly affecting the placenta. Any role that CT plays in the transport of calcium from mother to fetus has not been established.

The placenta is a temporary organ that joins the mother and fetus and functions to transfer nutrients and oxygen from the mother's blood into the blood of the fetus, as well as allowing the release of carbon dioxide and waste products from the fetus back to the mother (32). The placenta is different from other organs in that it is formed as a result of interaction between fetal and maternal tissues within the uterus. The placenta is located outside the fetal body and is connected by a cord of blood vessels. It is also an organ that has a limited lifespan and is disposable. Large differences exist between closely related species due to the fact that the placenta displays a wide variety of structural modifications (33).

The definitive placenta of most mammals is chorio-allantoic, whereby blood vessels of the mesodermal outer covering of the allantois form a vascular bridge between the embryo and the all-enveloping chorion (33). The human and murine placenta are structurally and functionally quite similar. For example, the chorio-allantoic placenta is the definitive type for both species, both have a placenta that is discoid in shape, and both placental membrane types are hemochorial (whereby the maternal blood comes in direct contact with the chorion). However, the murine placenta differs from the human placenta in that the murine placenta is hemotrichorial (has three layers of trophoblasts) whereas the human placenta is hemomonochorial (has one layer of trophoblasts) (34). Due to the functional similarities between the two species, the murine placenta serves as an excellent experimental model for study of the human placenta.

The placenta is composed of trophoblasts, which are the peripheral cells of the blastocyst that attach the fertilized ovum to the uterine wall and subsequently become the placenta and membranes that nourish and protect the developing embryo (32). Labyrinthine (or syncytial) trophoblasts, spongiotrophoblasts, and giant trophoblasts are the three types of trophoblasts found in the murine placenta. The bulk of the murine placenta is made up of the labyrinthine trophoblasts, which are considered to be the dominant site of maternal-fetal exchange, while the giant trophoblasts invade the decidual tissue and express several hormones (35).

The intraplacental yolk sac (IPYS) is a structure located in the rodent placenta which is often overlooked (Figure 2). The IPYS, which is generally considered to be a remnant of the primitive yolk sac, is found exclusively in rodent placentas. It is actually a bilayered membrane that is made up of tall columnar cells on the endothelial side overlaying fetal vessels and maternal blood spaces at the fetal pole of the placenta (35). Unlike an incorporated remnant, it actually invades, grows, and expands within the placenta during the latter half of gestation, always remaining situated between the fetal and maternal vessels (36) (Figure 3).

The actual mechanisms by which the active exchange of calcium occurs across the placenta are poorly understood. It is thought that calcium diffuses into calcium transporting cells through maternal facing basement membranes, is carried across these cells by calcium binding proteins, and is then actively expelled at the fetal facing basement membranes by Ca^{++}ATPase (the "calcium pump") (35). While the majority of calcium is transported actively, some calcium may pass from maternal to fetal

Figure 2. The intraplacental yolk sac (IPYS) in late gestation. Late in gestation, the yolk sac is compressed such that it completely lines the uterine cavity that is not in contact with the placenta and it overlies the dome of the placenta. The yolk sac bilayer that is overlying the dome of the placenta forms finger-like projections into the placenta near the insertion of the fetal vessels, and these projections are termed the IPYS. (From (35))

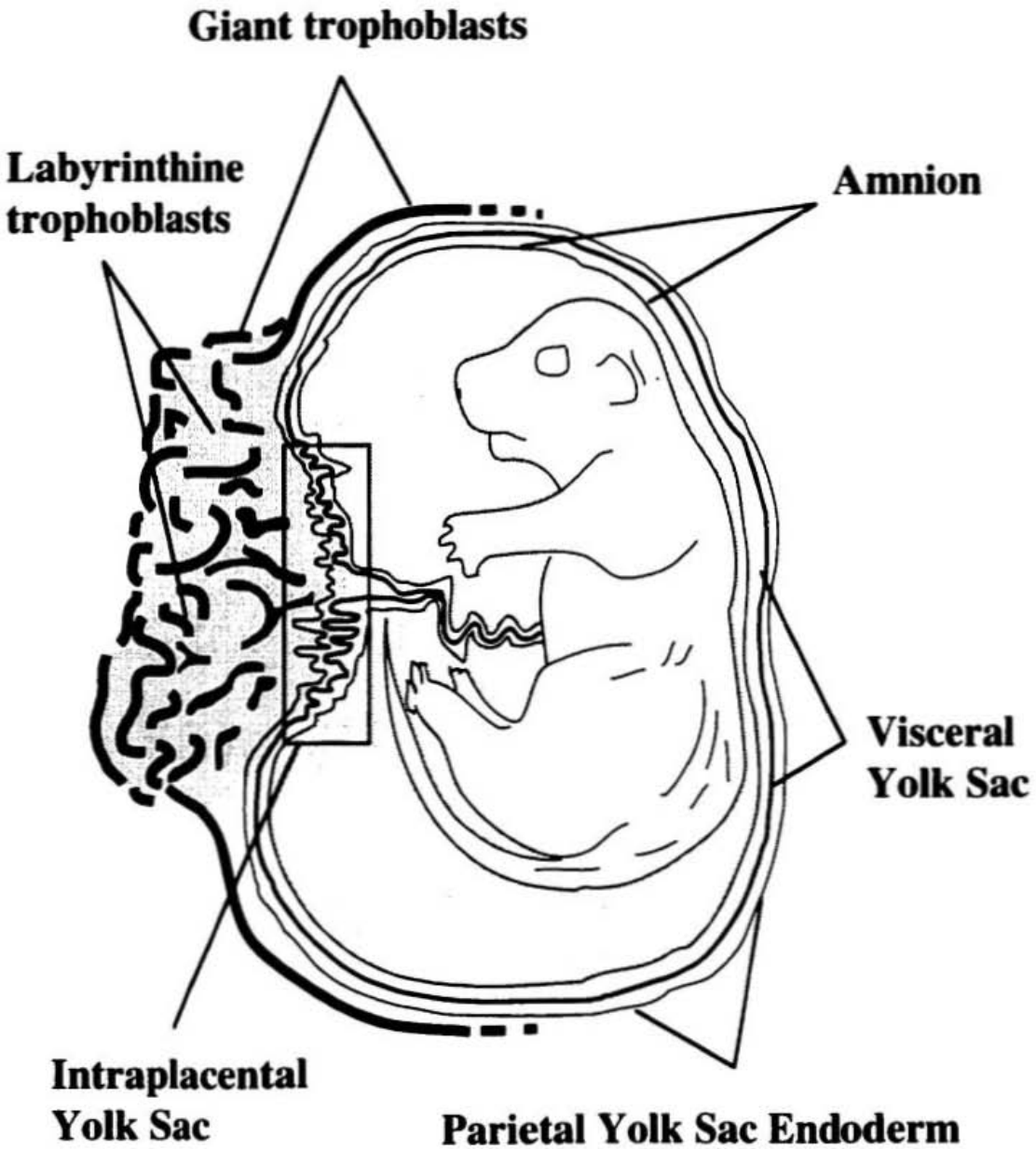
Giant trophoblasts
Labyrinthine trophoblasts
Amnion
Visceral Yolk Sac
Intraplacental Yolk Sac
Parietal Yolk Sac Endoderm

Figure 3. Detailed anatomy of the intraplacental yolk sac (IPYS). The IPYS is situated between the fetal and maternal blood spaces. The parietal layer and Reichert's membrane overlie maternal blood vessels whereas the visceral layer overlies the fetal blood vessels. The sinus of Duval is located between these layers and functions to communicate with the yolk sac cavity and the uterine lumen. (From (35)).

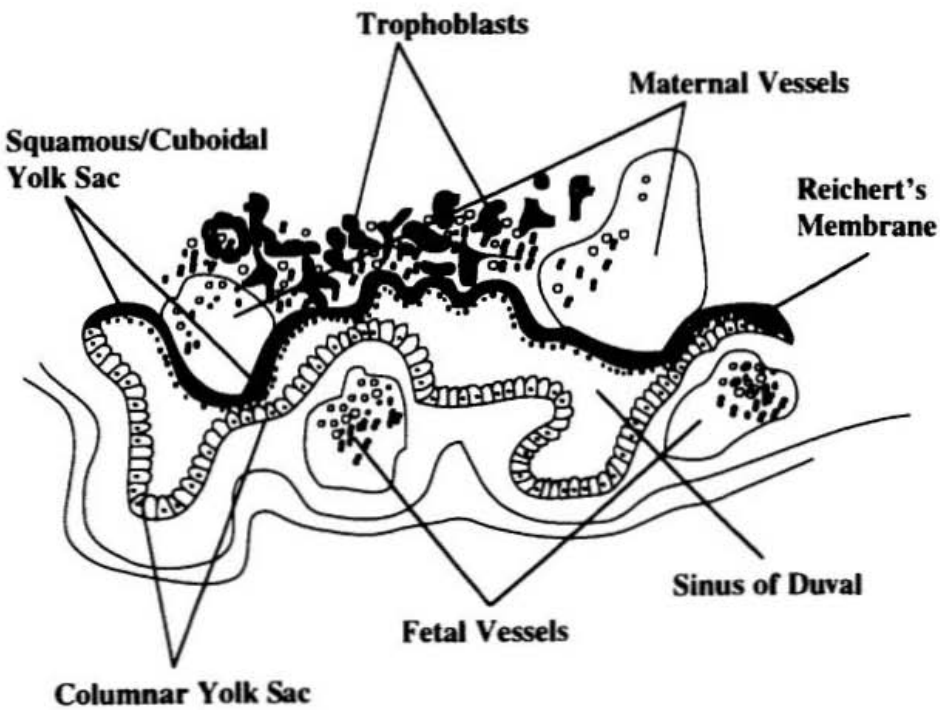
Trophoblasts
Maternal Vessels
Squamous/Cuboidal
Yolk Sac
Reichert's
Membrane
Sinus of Duval
Fetal Vessels
Columnar Yolk Sac

circulations by such processes as vesicular transport, paracellular transport, and simple diffusion (35). The site of active transport is most likely in the trophoblast cells and possibly in the endoderm of the IPYS in rodents. These cells are in closest proximity to the maternal circulation, and the IPYS cells express particularly high levels of Ca^{++}ATPase and calbindin-D_{9k} (a calcium binding protein).

1.8 Calcitonin/Calcitonin Gene-Related Peptide Knockout Mouse Model

The purpose of this project was to explore the role that CT plays in fetal-placental calcium and bone homeostasis. This was achieved by studying a CT knockout mouse model in which the gene for CT has been eliminated. Therefore, any effects in fetal calcium metabolism seen in this model could be attributed to the loss of the hormone. Until recently, there had not been an adequate model of experimental CT deficiency created, as previously described in sections 1.4 and 1.5.

The generation of a CT knockout mouse model by Hoff and others (37) provided a useful model for determining the precise role of CT in calcium and bone homeostasis. More specifically, it provides a fetal model for study that otherwise could not be created by surgical or pharmacological techniques. Mice deficient in CT were created by replacing exons 2 through 5 of the mouse CT1 gene with PGKneoBPA (these mice were not generated in our laboratory and therefore the details of their creation will not be discussed). Since exons 2 through 5 have been replaced, CGRP has also been knocked out, and therefore, these mice lack both CT and CGRP. However, for the purposes of this project, this mouse model will be considered to be simply a CT knockout.

Homozygous null mice for the CT1 gene were generated using standard techniques, are born normally, are fertile, and also live a normal lifespan. CT deletion was confirmed by molecular analysis of homozygous knockouts, as well as through the absence of immunohistochemical staining for CT in the thyroid gland of the homozygous animals. A report of how the loss of the hormone in these mice affects calcium and bone metabolism in the adult is the subject of a separate report by Hoff that has not yet been published.

1.9 Project Description and Purpose

This project specifically examined the role of CT in fetal-placental calcium and bone homeostasis. The previous work of others in this area has been complicated by the technical difficulties involved in physiological studies of the fetus, and of creating mice that are completely CT-deficient. The novel strategy used in these studies was to compare and contrast the physiological impact on fetal calcium homeostasis of the selective removal of the CT gene through gene targeting. Homozygous (HOM) CT gene-deleted mice have complete absence of the gene product, the hormone CT. Wild-type (WT) mice have both copies of the CT gene while heterozygous (HET) mice have one copy of the CT gene and one copy of the knockout gene.

HET males and females were mated together to create pregnancies in which WT, HET, and HOM fetuses were present. The HOM fetuses were compared (phenotypically and physiologically) to their WT siblings to determine if the fetal loss of CT has any impact on the fetus.

HET males and HOM females were also mated to generate pregnancies in which HOM and HET fetuses were present. The HOM fetuses of HOM dams were compared to their HET siblings and to the fetuses of HET mothers, to determine if the maternal loss of CT has any impact on the fetus.

By observing what happened as a result of the absence of CT in the mother or the fetus, these studies provided the opportunity to determine what role (if any) CT plays in normal fetal calcium and bone physiology

II GENERAL METHODS

2.1 Animal Husbandry

2.1.1 Animals

HET males and females were mated to create pregnancies in which WT, HET, and HOM fetuses were present. HET males and HOM females were also mated to yield pregnancies with HET and HOM fetuses. The HET and HOM females were first degree relatives of each other. The original homozygous knock-out mice were crossed into Black Swiss mice for several generations. Genotypes of mice were confirmed by polymerase chain reaction (PCR) of genomic DNA. Animals were maintained in facilities operated by Animal Care Services of Memorial University of Newfoundland, in accordance with the Canadian Council on Animal Care (CCAC). All protocols were approved by the Institutional Animal Care Committee (IACC).

2.1.2 Timed Matings

HET and HOM females were mated overnight with HET males. The gestational day 0.5 was marked by the presence of a vaginal mucous plug on the morning following mating. The normal mouse gestation period is 19 days and fetuses of gestational ages of usually 18.5 days were studied. Fetuses of day 17.5 gestational age were utilized for placental calcium transfer studies.

2.2 Genotyping

2.2.1 DNA Extraction

To genotype fetuses, the tail was clipped and placed in 500 µl of lysis buffer (100 mM Tris•HCl, pH 8.0 / 500 mM EDTA, pH 8.0 / 0.2% SDS/200 mM NaCl) containing 100 µg/ml of proteinase K and were incubated at 55 °C for 12-24 hours. In brief, genomic DNA was precipitated with isopropanol, resuspended in water, extracted with phenol-chloroform, followed by precipitation by ethanol. The DNA was generally resuspended in 50 µl of pH 8.0 Tris-EDTA buffer (10 mM Tris and 1 mM EDTA) and 1.5 µl of DNA was subsequently used for PCR. The DNA extraction procedure is outlined in detail in the Appendix.

2.2.2 Polymerase Chain Reaction

Genotyping was achieved by PCR using primers specific to the CT gene sequence in a single-tube 36-cycle PCR reaction. A three primer system was utilized and included primers for the retained portion of the WT allele (CT-1), a deleted portion of the WT allele (CT-3), and the inserted neomycin sequence (CT-N) (Figure 4A). These primers utilized the specific sequences: CAG GAT CAA GAG TCA CCG CT (CT-1), GGA GCC TGC GCT CCA GCG AA (CT-3), and GGT GGA TGT GGA ATG TGT GC (CT-N) (from GIBCO BRL, Burlington, Ontario).

PCR results were analyzed using gel electrophoresis. A 2% agarose gel was made (2 g agarose, 10 ml of 10x TAE {Tris-Acetic Acid-EDTA}, and 90 ml water), was

Figure 4. Genotyping by polymerase chain reaction (PCR). 4(A) A schematic of the normal and targeted CT allele with approximate locations of primers indicated. Mouse genotype was tested using two PCR reactions and 3 different primers. CT-1 is a primer to CT exon 1, which is present in normal and knockout animals. CT-3 is a reverse primer in intron 1 and CT-N is a reverse primer in the neomycin gene. 4(B) A schematic of the PCR product electrophoresed on an agarose gel, to demonstrate the typical results of a genotyping experiment. CT-1 and CT-3 primers are paired to detect the wild-type allele whereby the PCR product is approximately 250 base pairs. CT-1 and CT-N primers are paired to detect the knockout (homozygous) allele whereby the PCR product is approximately 150 base pairs (B). Wild-type = WT, homozygous = HOM, and heterozygous = HET.

A

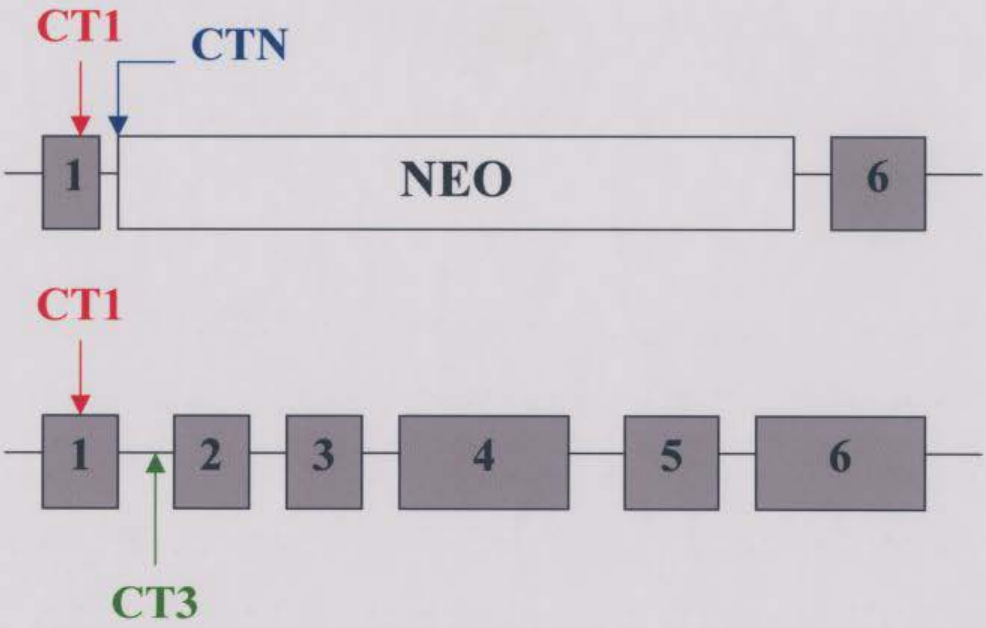

B

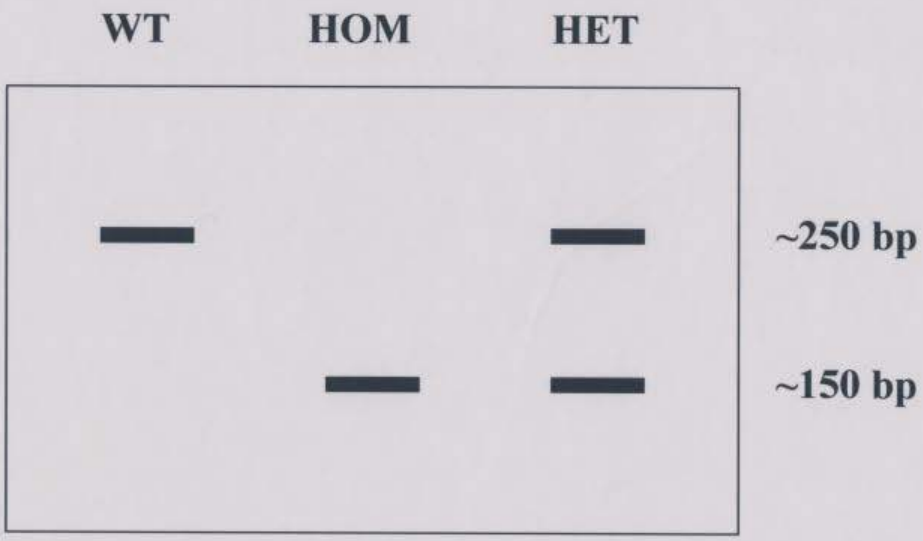

microwaved for two minutes, 6 µl of ethidium bromide was added, and was poured into a gel tray. 10 µl of each PCR product (combined with 2 µl of Orange G loading dye) was added to a well in the gel. The samples were run on the gel in an electrophoresis chamber at 200 volts for 25-30 minutes in 700 ml of 1xTAE buffer. Gel results were documented using a Multi Image Light Cabinet and Chemi Imager-4000 software package from Alpha Innotech Corporation (Canberra-Packard Canada Ltd., Montreal, Quebec). Genotypes were subsequently determined from the photographs. WT produces a 250 bp band, HOM produces a 150 bp band, while HET produces both 250 bp and 150 bp bands (showing both the WT and HOM alleles) (Figure 4B).

2.3 Data Collection

2.3.1 Litter Sizes

At the time of each cesarian section (day 17.5 or 18.5 of gestation), the number of fetuses present were counted to determine the litter size. This number would be higher than the litter sizes observed 6-24 hours after birth, due to normal loss of pups in the period after birth.

2.3.2 Whole Blood and Serum Collection

On day 18.5 of pregnancy, dams were anesthestized by isoflurane (Janssen, Toronto, Ontario) inhalation and whole blood was collected from the heart using a 26 gauge needle and syringe. Pregnant dams were euthanized by rapid cervical dislocation.

The fetuses were quickly removed (to minimize changes in maternal/fetal blood chemistry) by cesarian section, leaving the uterus intact. Each individual fetus was removed from its amniotic sac, and the left carotid and jugular vessels were transected using a razor blade. For serum collection, approximately 40-75 µl of whole blood was collected from each fetus into plain capillary tubes. The samples were then separated by centrifugation and serum was stored at –20 °C until used for study.

2.3.3 Placental Perfusion

Placentas were obtained for study following placental perfusion with paraformaldehyde, to minimize mRNA or protein degradation which could occur during the fixation and processing of the RNase and protease-rich placental tissues. In brief, dams (at day 18.5 of pregnancy) were anaesthetized with isoflurane and a thoracotomy was performed. A 23 gauge needle was inserted into the left ventricle of the heart and the right ventricle was cut open to allow for drainage. 10 ml of 1x PBS (phosphate buffered saline) was slowly perfused into the heart. After most of the blood was flushed out, 10 ml of 4% paraformaldehyde was perfused into the heart. Following perfusion, the placentas were removed and placed in 10% formalin, and subsequently processed, embedded in paraffin, cut into 5 µm sections, and placed onto slides (using standard techniques). A detailed procedure is provided in the Appendix. The placental genotype was determined from the fetal tail DNA.

2.3.4 Tissue Preparation

Fresh tissue samples were obtained from fetuses of HET x HET matings that delivered at day 18.5 of gestation. For histology, fetuses were fixed in 10% buffered formalin. Following fixation, fetal tibias and femurs were removed from hind limbs, processed, embedded in paraffin and sectioned at 5 μm thick using standard techniques.

2.3.5 Amniotic Fluid Collection

Amniotic fluid is very scanty and viscous on day 18.5 of gestation, therefore, amniotic fluid was collected from day 16.5 and 17.5 fetuses. Each pregnant dam was killed by cervical dislocation and the intact uterus was removed by cesarian section. Each gestational sac was subsequently lanced, and 40-75 μl of fluid was collected into heparinized capillary tubes. The amniotic fluid was then decanted into storage tubes and frozen at –20 °C. Fetal tail clippings were taken for subsequent genotyping.

2.4 Placental Calcium Transfer

The rate of placental calcium transport was measured in accordance with the procedure previously developed by Kovacs et al. (9). On day 17.5 of gestation, pregnant dams were anesthestized by isoflurane inhalation. These mice were then given 50 μCi of ^{45}Ca and 50 μCi of ^{51}Cr-EDTA (in 0.9% saline) by intracardiac injection (the total volume injected was 100 μl). ^{51}Cr-EDTA crosses the placenta by diffusion only and was used as a blood diffusional marker to control for blood flow differences between placentas. The dams were euthanized five minutes after the injection by cervical dislocation. A five

minute time point was used to minimize the possibility of calcium backflux from fetus to mother. The intact uterus was removed from the mouse by cesarian section and each fetus was removed from its amniotic sac. The tail of each fetus was clipped for subsequent genotyping, and each fetus was placed in a test tube and asphyxiated. The amount of ^{51}Cr activity was measured using a gamma counter and the fetuses were then solubilized with 10 ml of Scintigest (Fisher Scientific, New Jersey) at 55°C for 48 hours and then were vortexed to disperse the tissues. When the fetuses were fully solubilized, 10 ml of scintillation fluid was added, along with 5 drops of glacial acetic acid (to minimize bioluminescence and chemoluminescence). The vials were then shielded from light and equilibrated to room temperature for 12-24 hours. A beta counter was used to measure ^{45}Ca activity and the ratio of $^{45}Ca/^{51}Cr$ activity was calculated for each fetus.

2.5 Mineral assays

2.5.1 Ionized calcium

Whole blood was collected from the tail vein of dams on day 18.5 of pregnancy into 50 µl heparinized capillary tubes which were capped and subsequently placed on ice. Fetal blood was normally collected on day 18.5 gestation so as to maximize the amount that could be collected. The pregnant mouse was euthanized by rapid cervical dislocation and the fetuses were quickly removed by cesarian section (to minimize changes in maternal/fetal blood chemistry), leaving the uterus intact. Each individual fetus was removed from its amniotic sac, and the left carotid and jugular vessels were transected

using a razor blade. Approximately 30-50 µl of whole blood was collected into 50 µl heparinized capillary tubes, a volume sufficient for one ionized calcium measurement. The capillary tubes were capped and immediately placed on ice and the order that each fetus collected in the litter was recorded. The tail of each fetus was subsequently clipped, placed in lysis buffer, whereby DNA was later extracted for PCR genotyping. Each fetal and maternal blood sample was analyzed for the ionized calcium and pH on a CIBA/Corning 634 Ca^{++}/pH analyser (with a measurement range of 0.20 mmol/L to 5.00 mmol/L for Ca^{++} and 6.00 to 8.00 for pH). The raw ionized calcium values were used for analysis.

2.5.2 Serum Magnesium

The magnesium content of fetal serum was determined using a Magnesium Kit from Sigma Diagnostics (St. Louis, MO). This procedure was carried out as directed in the package insert (Appendix).

2.5.3 Serum Phosphorus

The inorganic phosphorus content of fetal serum was determined using an Inorganic Phosphorus Kit from Sigma Diagnostics (St. Louis, MO). This procedure was carried out as directed in the package insert (Appendix).

2.5.4 Fetal Ash Weights

Each genotyped fetus was weighed, placed in a crucible and reduced to ash in a Thermolyne Type F62700 furnace for 24 hours. The ash was then dusted onto weighing paper and each sample was weighed. The ash weight of each fetus reflects the total mineral content of the fetal skeleton.

2.5.5 Flame Atomic Absorption Spectroscopy

Fetal skeletal calcium and magnesium content were analyzed using atomic absorption spectroscopy. 253 µl of ultra pure nitric acid was added to fetal ash collected in sample vials. The samples were then allowed to dissolve at room temperature for 3 days. 10 ml of distilled water was added to each vial, dilutions were made, and samples were run in duplicate on a Perkin-Elmer 2380 Atomic Absorption Spectrometer. Results were converted to mg/g of ash.

2.6 Calciotropic Hormone Assays

2.6.1 PTH ELISA

The PTH content of fetal serum was determined using a Rat 1-34 Intact PTH ELISA (Enzyme-Linked ImmunoSorbent Assay) Kit from Immutopics (San Clemente, CA). The procedure was carried out as outlined in the kit protocol (Appendix). However, in cases where sample serum volumes were less than 25 µl, samples were diluted with 0 pg/ml Standard.

2.6.2 Rat CT IRMA

The CT content of maternal and fetal serum was determined using a Rat CT IRMA (Immunoradiometric Assay) Kit from Immutopics (San Clemente, CA). The procedure was carried out as outlined in the kit protocol (Appendix). However, 100 µl of pooled serum plus 100 µl of Sample Diluent reagent was used for each fetal sample. No pooling was required for maternal serum samples.

2.7 Skeletal and Placental Histology and Morphology

2.7.1 *In situ* Hybridization

For *in situ* hybridization on fetal placental sections, ^{35}S-riboprobes for CT, calbindin-D_{9k} and Ca^{++}ATPase were prepared. For *in situ* hybridization on fetal bone, ^{35}S-riboprobes for collagen I, collagen II, collagen X, cartilage matrix protein (CMP), histone-4, alkaline phosphatase, osteocalcin, 92-kD gelatinase, PTHrP, collagenase-3, and osteopontin were prepared. The specific probes used were generated from the appropriated cDNAs whereby the generation of labelled strands which are complementary to the cDNA are antisense probes. The detailed *in situ* hybridization procedure is provided in the Appendix. Essentially, the procedure involves the linearization and purification of plasmids, labelling of riboprobes, prehybridization treatment of slides, application of the probe cocktail, posthybridization washes, autoradiography, staining, and photography. Bright field and/or dark field microscopy were used to examine results whereby comparisons were made between WT and HOM

mice from the same litters and specimens had been treated under the same experimental conditions. Results were interpreted based on the intensity and location of mRNA expression.

2.7.2 Immunohistochemistry

Immunohistochemistry was performed on 5 μm placental sections using two particular antibodies; anti-CT (DAKO, Denmark) was used at 1:200 dilution and anti-CT-receptor (courtesy of P. Wookey, University of Melbourne, Australia) was used at 1:500 dilution. Both antibodies were used with secondary antibody, ABC reagent, and DAB-Tris-peroxidase kits obtained from Vector (Burlington, Ontario). Slides containing placental sections were incubated in 1.0% H_2O_2 in methanol (to inactivate endogenous peroxidases) for 30 minutes at room temperature, and incubated with 100 μl of blocking serum for 20 minutes (to saturate cellular F_c receptors). Following this, slides were incubated with 100 μl of the primary antibody at 4 °C overnight for the CT antibody and for one hour at room temperature for the CTR antibody. Next, 100 μl of biotinylated secondary antibody was applied to each section for 30 minutes, followed by incubation with DAB-Tris-peroxidase for 10 minutes and counter-stained with Contrast Red (Kirkegard and Perry Laboratories, Gaithersburg, Maryland) for 5 minutes and subsequently washed, dehydrated, and mounted with Permount (Fisher Scientific Company, Fair Lawn, New Jersey) and a coverslip was applied. Staining intensity was determined using bright field microscopy in a blind manner whereby the genotype was not known. These results were confirmed on at least 2 separate litters.

2.7.3 Alizarin Red S and Alcian Blue Staining:

Day 18.5 fetuses were fixed in 95% ethanol for at least 5 days. Skin, viscera, and adipose tissue were removed within 2 hours of death. A detailed protocol is provided in the Appendix. In brief, the fetuses were placed in acetone for at least 2 days in order to remove fat and keep the specimen firm, stained for 3 days in staining solution at 37 °C, and washed in water. Following this, fetuses were cleared in 1% aqueous KOH for 12-48 hours and subsequently in 20%, 50%, and 80% glycerol / 1% aqueous KOH solutions. Specimens were stored in 100% glycerin. As a result of this procedure, alizarin red stained bone red and alcian blue stained cartilage blue.

2.7.4 Von Kossa's Staining

This procedure is described in detail in the Appendix. In brief, fetal bone tissue sections were deparaffinized, rehydrated in decreasing concentrations of ethanol (100%, 100%, 95%, and 75%) and then equilibrated in distilled water. The sections were then placed in 1% aqueous silver nitrate solution and exposed to strong light for a 45 minute period. The sections were then washed three times in distilled water, treated for 5 minutes with 2.5% sodium thiosulfate and washed with distilled water again. Subsequently, the sections were counter-stained for 2 minutes with methyl green, rinsed in 1-butanol three times, dehydrated, and mounted with Permount.

2.8 Statistical Analysis

Data were analyzed using SYSTAT 5.2.1 for MacIntosh (SYSTAT, Evanston, IL.). ANOVA (analysis of variance) was used for all data analysis. Two-tailed probabilities are reported and all data are presented as mean ± SE. $P < 0.05$ was considered statistically significant.

For studies with results that may have been influenced by non-genotypic factors, including numbers of fetuses in the litter and size of fetuses, the data were normalized. The mean HET result for each litter was set at 100%, and HOM and WT results were expressed as a percentage of this HET mean. This method was used to normalize values among the pups of each litter so that comparisons may be made between different litters. Results were normalized to the HET mean since the HET genotype occurs at twice the frequency of either the WT or HOM, corresponding to the Mendelian ratio of 1:2:1. Since HET fetuses make up 50% of the total fetuses, the normalized value is more stable. Also, HET fetuses have both WT and HOM alleles and therefore should present an intermediate phenotype.

III RESULTS

3.1 Maternal Effects of CT Deletion

We measured litter size, maternal ionized calcium levels, and compared pregnant and nonpregnant HET and HOM females, in order to determine if there were any maternal effects of CT deletion.

HET males and females were mated to create pregnancies in which WT, HET, and HOM fetuses were present. HET males and HOM females were also mated to yield pregnancies with HET and HOM fetuses. The HET and HOM females were first degree relatives of each other in order to ensure that comparisons are made between mice of the same genetic background. The *in utero* litter size of HOM females was significantly lower than that of HET females (7.89 ± 0.39 pups [28 litters] vs. 9.12 ± 0.31 pups [43 litters], respectively; p=0.017) (Figure 5).

We measured maternal serum ionized calcium levels and compared pregnant and nonpregnant HET and HOM females. Maternal blood was obtained from tail veins on day 18.5 of gestation. Maternal calcium levels were 1.28 ± 0.02 mmol/l in HET and 1.29 ± 0.02 mmol/l in HOM dams (p=NS, and no different from the corresponding nonpregnant maternal values) (Figure 6).

In summary, maternal loss of CT affected litter size but had no effect on maternal blood calcium.

Figure 5. Comparison of *in utero* fetal number (mean ± SE) of HET and HOM dams.

The number of observations is indicated in parentheses.

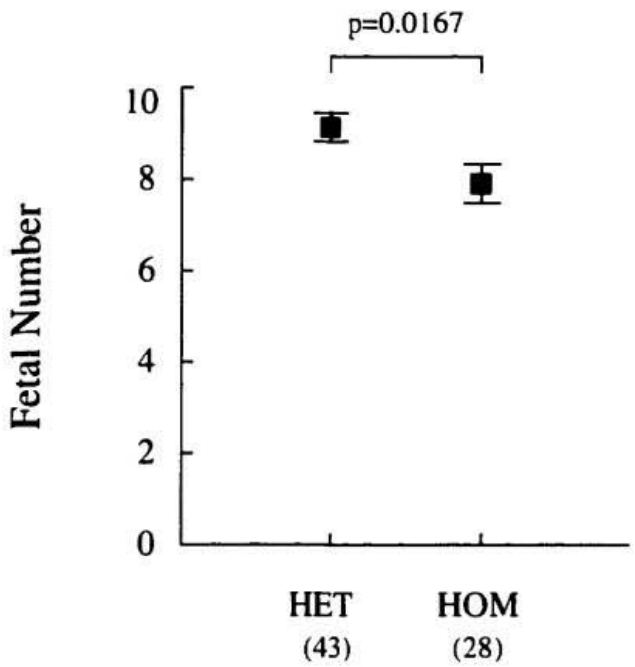
p=0.0167
Fetal Number
10
8
6
4
2
0
HET
(43)
HOM
(28)

Figure 6. Ionized calcium levels (mean ± SE) in pregnant versus non-pregnant HET and HOM female mice (p=NS). The number of observations is indicated in parentheses.

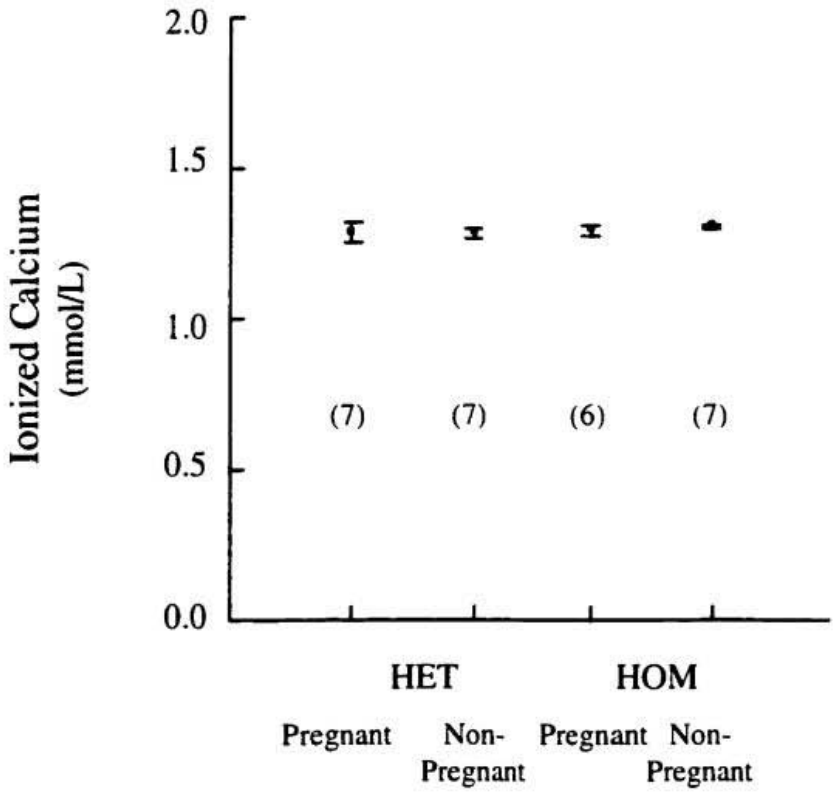
Ionized Calcium
(mmol/L)
2.0
1.5
1.0
0.5
0.0
(7)
(7)
(6)
(7)
HET
HOM
Pregnant
Non-
Pregnant
Pregnant
Non-
Pregnant

3.2 Placental Calcium Transport

The fetus and placenta must obtain sufficient calcium to mineralize the skeleton, and maintain an extra-cellular level of calcium that is physiologically appropriate for fetal tissues. Maternal hormones might influence fetal-placental calcium transport by raising or lowering the ambient maternal calcium level and by direct effects on the placenta. We measured the rates of calcium transport across the placenta to the fetuses of both HET and HOM dams. Placental calcium transfer was assessed by administering ^{45}Ca and ^{51}Cr (as a diffusional marker) to the pregnant dam, by intracardiac injection, on day 17.5 gestation. The amount of ^{45}Ca transferred to each fetus within 5 minutes (normalized by ^{51}Cr) did not differ among fetuses of HET dams (96.01 ±8.24% in HOM fetuses, 101.29 ±6.08% in HET fetuses, and 102.37 ±7.81% in WT fetuses; p=0.83) (Figure 7A). No significant differences between HET and HOM fetuses of HOM dams were found (99.83 ±4.47% and 94.93 ±4.30% respectively; p=0.43) (Figure 7B).

Thus, it appears that neither fetal nor maternal loss of CT affects the rate of transport of calcium across the placenta from mother to fetus.

3.3 Mineral Physiology

Ninety-nine percent of the body's calcium and most of its magnesium resides in the skeleton. We measured the content of these minerals in the skeletons of fetuses of HET and HOM dams. We also measured serum levels of calcium, magnesium, and phosphorous because the regulation of calcium metabolism is often linked to phosphorous metabolism, and to a lesser extent, magnesium metabolism.

Figure 7. Placental calcium transport of ^{45}Ca and ^{51}Cr-EDTA in fetuses of HET (A) and HOM (B) dams. The ratio of ^{45}Ca /^{51}Cr activity was determined 5 minutes after maternal administration of the isotopes. Results were normalized to the mean HET value for each litter (p=NS). The number of observations is indicated in parentheses.

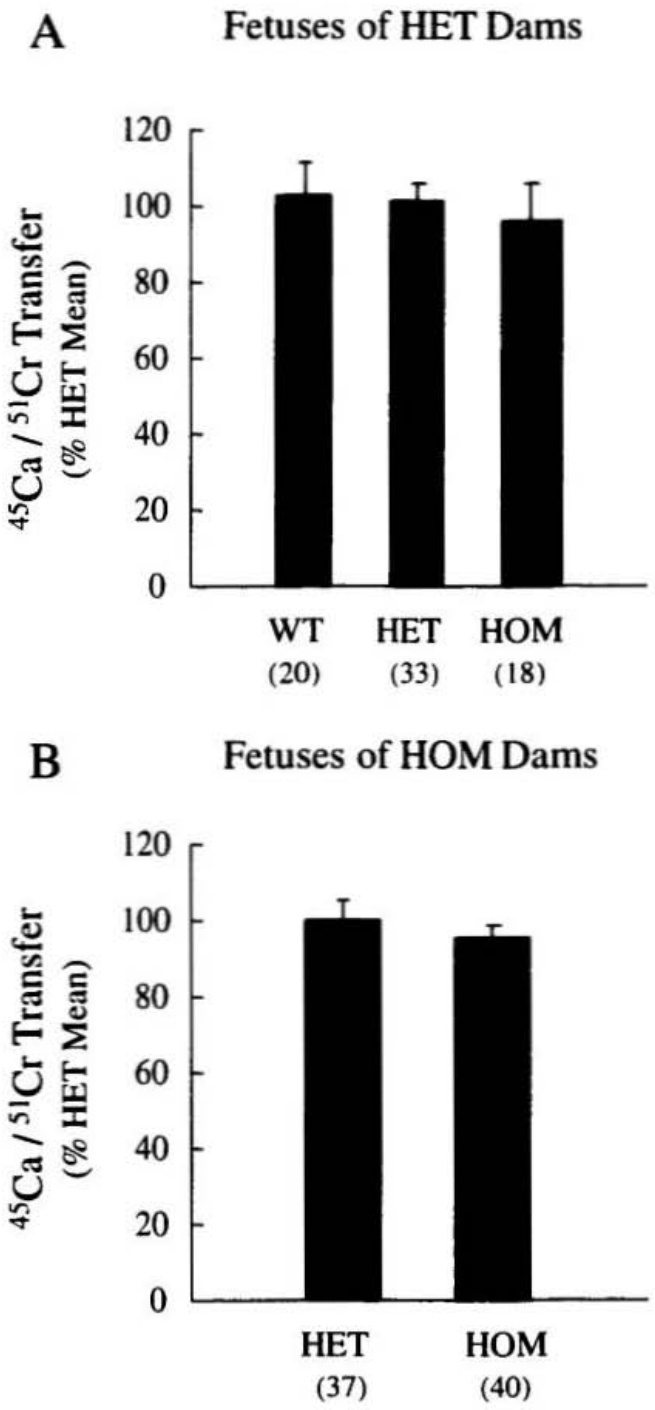
A
Fetuses of HET Dams
^{45}Ca / ^{51}Cr Transfer
(% HET Mean)
120
100
80
60
40
20
0
WT
(20)
HET
(33)
HOM
(18)
B
Fetuses of HOM Dams
^{45}Ca / ^{51}Cr Transfer
(% HET Mean)
120
100
80
60
40
20
0
HET
(37)
HOM
(40)

We measured ionized calcium levels of WT, HET, and HOM fetuses of HET dams. To determine if maternal loss of CT had any effect on fetal calcium, we also measured ionized calcium of fetuses of HOM dams. As well, in all mammals that have been studied, the fetal blood calcium (both total and ionized) is maintained at a higher level than in the maternal circulation and is believed to result, in part, from the active transport of calcium across the placenta. However, the physiological importance of fetal hypercalcemia is not known. Thus, we compared the amount of ionized calcium in maternal circulation to that in fetal circulation in these knockout mice to determine whether the loss of CT has any effect on the fetal-maternal calcium gradient. Fetal blood was collected by carotid/jugular transection, on day 18.5 of gestation (one day before expected birth). HOM fetuses exhibited a normal fetal-maternal calcium gradient with a fetal ionized calcium that did not differ from their HET or WT siblings, and did not differ by the mother's genotype (1.59 ± 0.02 mmol/l in HOM fetuses from HOM dams vs. 1.63 ± 0.01 mmol/l in HOM fetuses from HET dams, p=NS) (Figure 8).

Magnesium levels were measured in serum of fetuses of both HET and HOM dams. Serum magnesium levels of HOM fetuses of HET dams were significantly lower than that of their WT siblings (0.58 ± 0.10 mmol/L vs. 1.08 ± 0.10 mmol/L, respectively; $p<0.006$) (Figure 9A). Also, HOM fetuses of HOM dams had significantly lower serum magnesium levels than their HET littermates (0.86 ± 0.03 mmol/L vs. 1.01 ± 0.03 mmol/L, respectively; $p<0.004$) (Figure 9B). Serum phosphorous levels did not differ among fetuses of HET dams (1.64 ±0.30 mmol/L in HOM fetuses, 2.42 ±0.21 mmol/L in HET fetuses, and 2.36 ±.30 mmol/L in WT fetuses; p=0.11) (Figure 10A) and HOM dams

Figure 8. Ionized calcium levels (mean ± SE) of fetuses from HET (A) and HOM (B) dams (p=NS). The number of observations is indicated in parentheses.

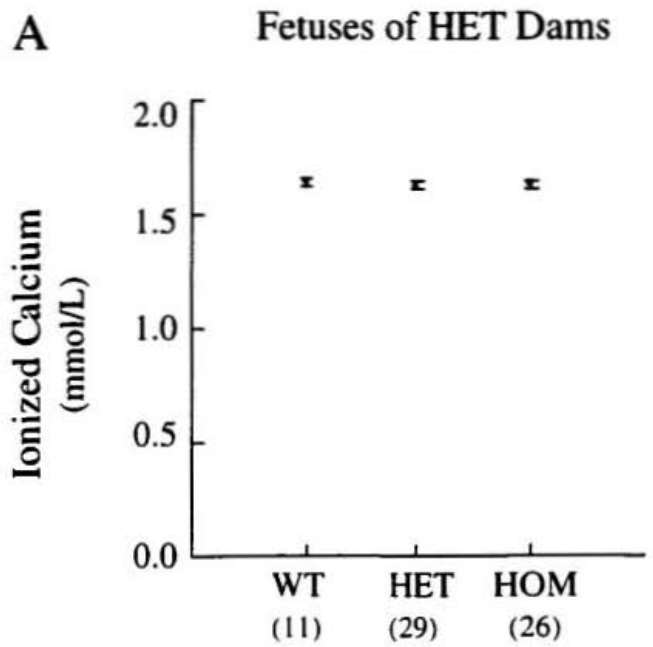
A
Fetuses of HET Dams
Ionized Calcium
(mmol/L)
2.0
1.5
1.0
0.5
0.0
WT
(11)
HET
(29)
HOM
(26)

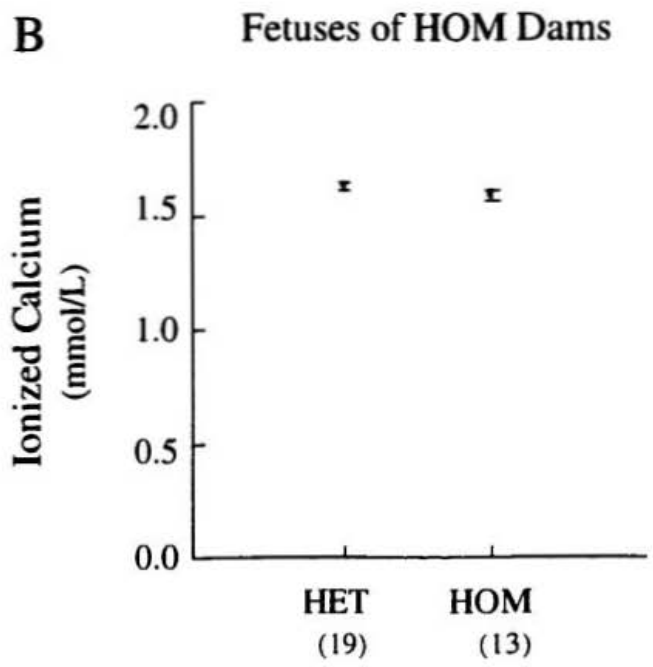
B
Fetuses of HOM Dams
Ionized Calcium
(mmol/L)
2.0
1.5
1.0
0.5
0.0
HET
(19)
HOM
(13)

Figure 9. Serum magnesium levels in fetuses of HET (A) and HOM (B) dams. Fetal serum magnesium was significantly reduced (p=0.0063) in HOM fetuses of HET dams, as compared to WT littermates. Serum magnesium was significantly reduced (p=0.0037) in HOM fetuses of HOM dams, compared to HET littermates. The number of observations is indicated in parentheses.

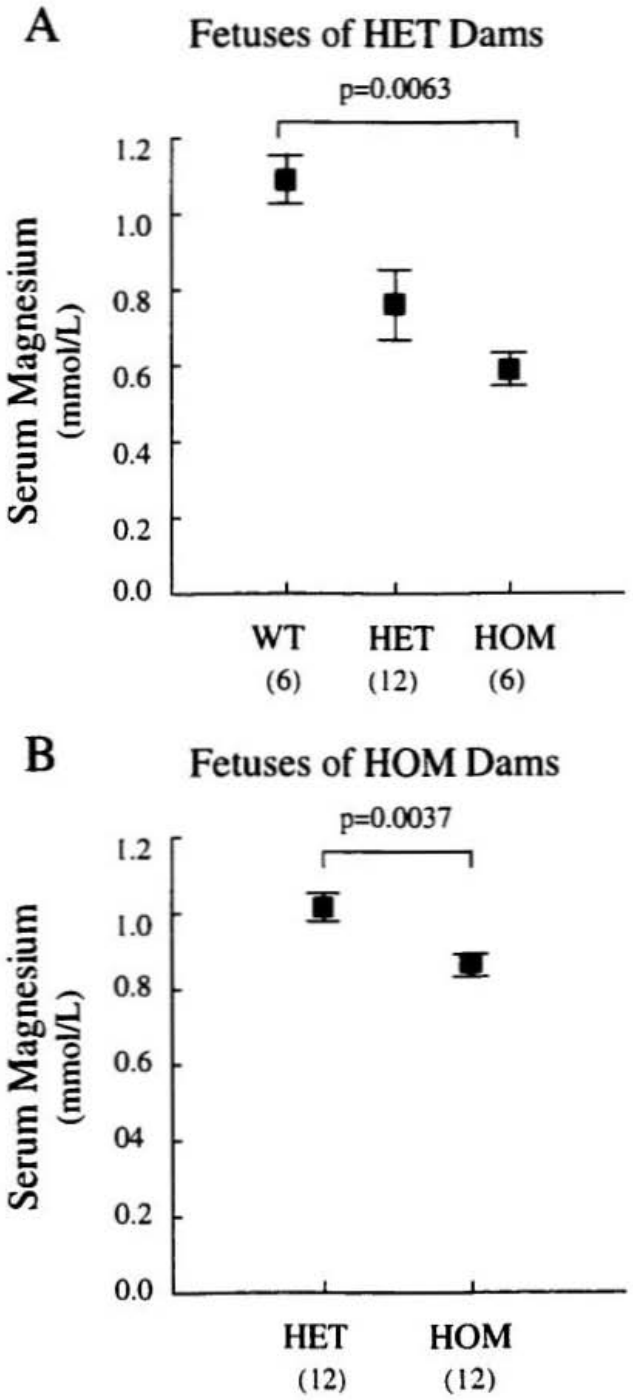
A
Fetuses of HET Dams
p=0.0063
Serum Magnesium
(mmol/L)
1.2
1.0
0.8
0.6
0.4
0.2
0.0
WT
(6)
HET
(12)
HOM
(6)
B
Fetuses of HOM Dams
p=0.0037
Serum Magnesium
(mmol/L)
1.2
1.0
0.8
0.6
04
0.2
0.0
HET
(12)
HOM
(12)

Figure 10. Serum phosphorus levels in fetuses of HET (A) and HOM (B) dams (p=NS).

The number of observations is indicated in parentheses.

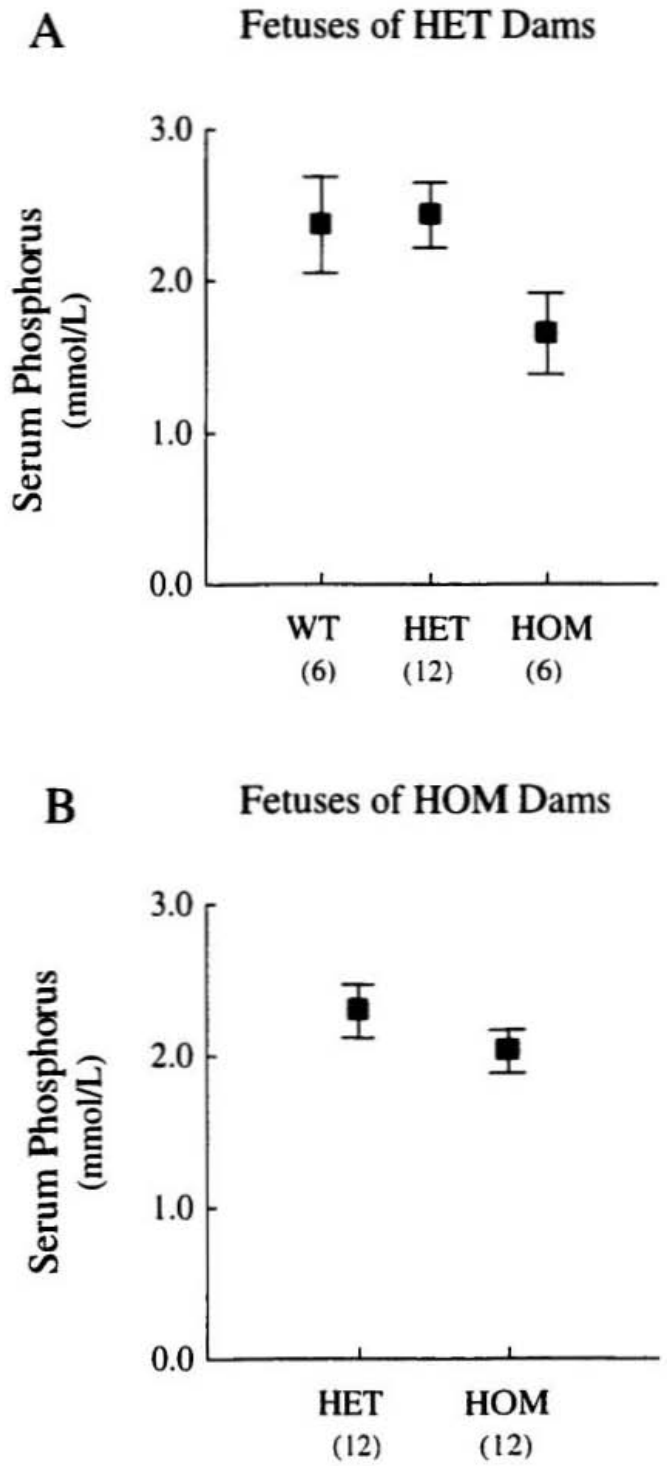
A
Fetuses of HET Dams
Serum Phosphorus
(mmol/L)
3.0
2.0
1.0
0.0
WT
(6)
HET
(12)
HOM
(6)
B
Fetuses of HOM Dams
Serum Phosphorus
(mmol/L)
3.0
2.0
1.0
0.0
HET
(12)
HOM
(12)

(2.02 ±0.15 mmol/L in HOM fetuses vs. 2.28 ±0.15 mmol/L in HET fetuses; p=0.24) (Figure 10B). HOM serum phosphorus levels trended lower but were not significantly different.

We measured the gross skeletal mineral present at the end of gestation by determining the ash weights of fetuses. Fetuses of both HET and HOM dams were ashed at 500°C for a period of 24 hours. The ash weights of fetuses were calculated and normalized to the mean heterozygote value for each litter. No differences were found in ash weights of HOM fetuses of HET dams compared to HET and WT littermates (102.40 ±2.95% in HOM fetuses, 100.05 ±2.00% in HET fetuses, and 97.66 ±3.31% in WT fetuses; p=0.57) (Figure 11A). We also compared ash weights of HOM to HET fetuses of HOM dams. No significant differences were found (100.13 ±1.78% in HOM fetuses vs. 100.02 ±2.19%; p=0.97) (Figure 11B).

The fetal ash was further analyzed by atomic absorption spectroscopy to more specifically quantify the amount of calcium and magnesium present and thereby determine whether the loss of CT affected the total skeletal calcium and magnesium content. Results were calculated in mg/g of ash and normalized to the mean heterozygote value for each litter. Total skeletal calcium of HOM fetuses of HET dams did not differ from their HET and WT siblings (97.59 ±4.09% in HOM fetuses, 100.02 ±2.89% in HET fetuses, and 101.89 ±4.72% in WT fetuses; p=0.78) (Figure 12A). Total skeletal calcium of HOM fetuses of HOM dams did not differ from their HET littermates (101.96 ±1.17% in HOM fetuses vs. 99.99 ±1.42% in HET fetuses; p=0.29) (Figure 12B). Total skeletal magnesium of HOM fetuses of HET dams did not differ from their siblings (97.65

Figure 11. Gross skeletal mineral present at the end of gestation is represented by the relative ash weights of fetuses of HET (A) and HOM (B) dams. Results are expressed as a percentage of the HET mean (p=NS). The number of observations is indicated in parentheses.

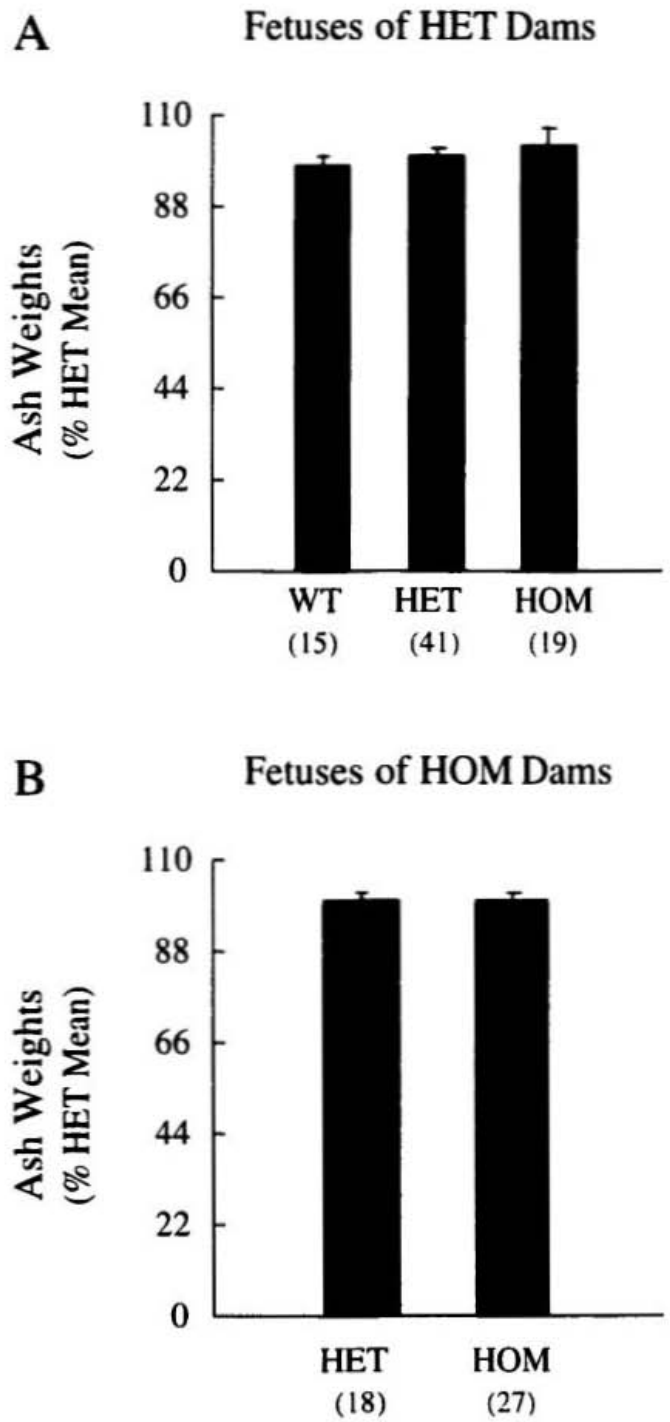
A
Fetuses of HET Dams
Ash Weights
(% HET Mean)
110
88
66
44
22
0
WT
(15)
HET
(41)
HOM
(19)
B
Fetuses of HOM Dams
Ash Weights
(% HET Mean)
110
88
66
44
22
0
HET
(18)
HOM
(27)

Figure 12. Determination of skeletal calcium content by atomic absorption spectroscopy in fetuses of HET (A) and HOM (B) dams. Results were calculated in mg/g of ash and normalized to the mean HET value for each litter (p=NS). The number of observations is indicated in parentheses.

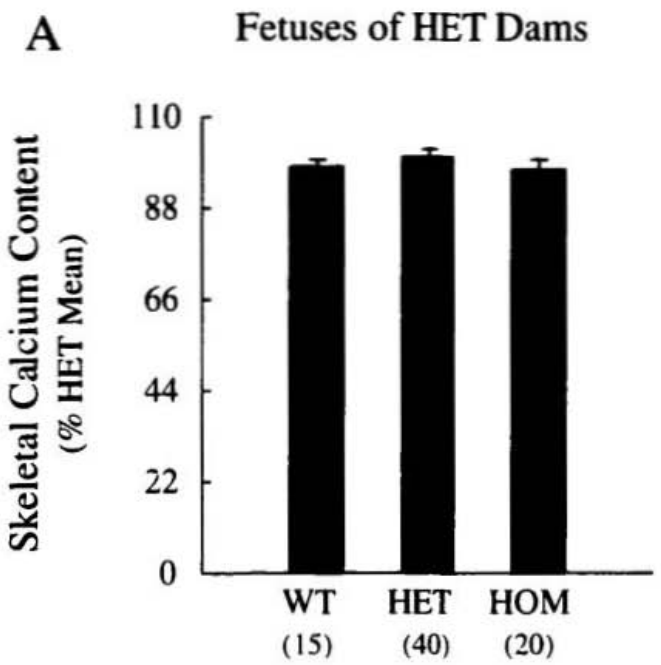
A
Fetuses of HET Dams
Skeletal Calcium Content
(% HET Mean)
110
88
66
44
22
0
WT
(15)
HET
(40)
HOM
(20)

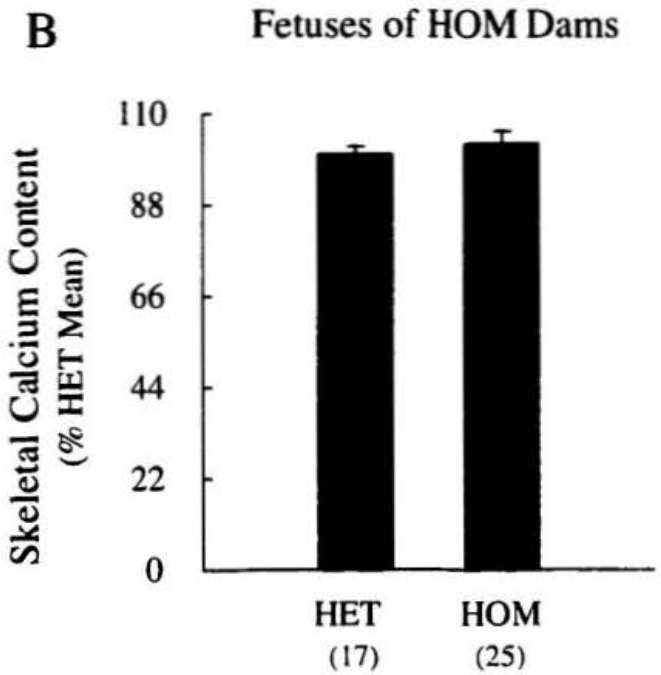
B
Fetuses of HOM Dams
Skeletal Calcium Content
(% HET Mean)
110
88
66
44
22
0
HET
(17)
HOM
(25)

±3.59% in HOM fetuses, 100.07 ±2.54% in HET fetuses, and 100.36 ±4.15% in WT fetuses; p=0.84) (Figure 13A). However, a trend was found between the total skeletal magnesium of HOM fetuses compared to HET fetuses (93.39± 2.58% and 100.08 ± 2.13% respectively; p=0.0527) (Figure 13B).

In summary, loss of fetal or maternal CT caused a reduction in the concentration of magnesium in the fetal circulation and possibly in the fetal skeleton. However, fetal serum calcium and phosphorus, and skeletal calcium content were not affected.

3.4 The Fetal Skeleton

Fetal bones were studied since bone is a compartment which is intimately involved in calcium metabolism and it mineralizes in late gestation. Therefore, disruption of calcium homeostasis and especially placental calcium transfer could result in altered skeletal development, altered skeletal mineral content, or altered gene expression in the growth plate.

The gross morphology and mineralization of the fetal skeleton were studied using alcian blue and alizarin red S staining. This procedure allows us to visually observe the morphology of the skeleton, as well as the relative amount and distribution of cartilage and mineralized tissue that is present. Using this procedure, the soft tissues become transparent and the entire skeleton (cartilaginous and mineralized portions) can be visualized. Alizarin red stains mineralized tissue (such as bone) red whereas alcian blue stains cartilage blue. No apparent differences were found when comparing the amount and distribution of bone and cartilage staining of HOM fetuses to their WT littermates,

Figure 13. Determination of skeletal magnesium content by atomic absorption spectroscopy in fetuses of HET (A) and HOM (B) dams. Results were calculated in mg/g of ash and normalized to the mean HET value for each litter. Skeletal magnesium content in HOM fetuses of HOM dams was reduced by 7% (p=0.0527). There were no differences found between fetuses of HET dams. The number of observations is indicated in parentheses.

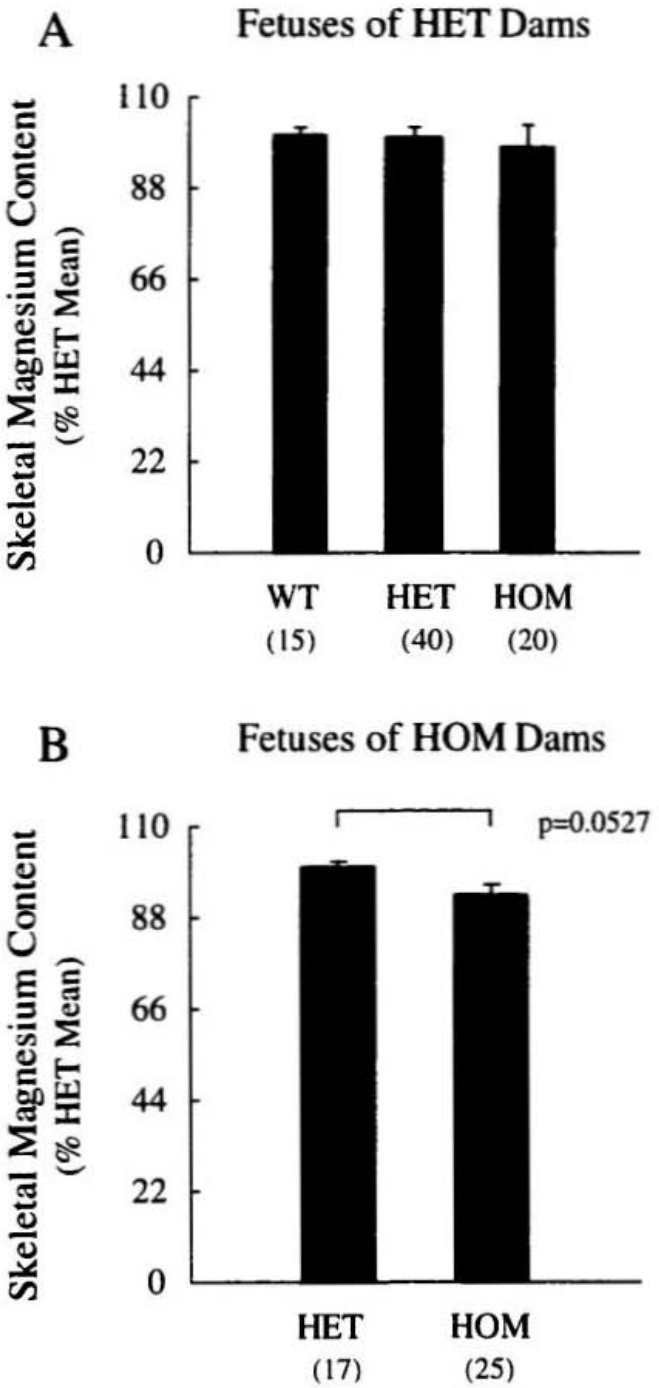
A
Fetuses of HET Dams
Skeletal Magnesium Content
(% HET Mean)
110
88
66
44
22
0
WT
(15)
HET
(40)
HOM
(20)
B
Fetuses of HOM Dams
Skeletal Magnesium Content
(% HET Mean)
110
88
66
44
22
0
p=0.0527
HET
(17)
HOM
(25)

nor did there appear to be any morphological differences between the fetal skeletons, such as the length and shape of the long bones (Figure 14).

The amount of bone mineral present in the growth plates of fetal bones was further studied using the von Kossa method. In this method, mineral is blackened by silver phosphate and silver carbonate complexes. This method detects inorganic phosphates and carbonates, however, since calcium is the only cation that binds to inorganic phosphate and carbonate anions in living tissues, this method is also considered to be an indirect but specific test for the presence of calcium (38) (39). Using this method, the amount of mineral present in HOM fetal bones did not differ from that of their WT siblings (Figure 15).

In situ hybridization was performed on fetal bone sections to determine whether the expression of important markers of bone development and cell type are altered in the absence of CT. mRNA expression of markers for the various cellular regions of the growth plate were studied. A detailed list of the mRNAs that were studied is provided in Table 1, however only results for those probes which produced clear and consistent results are reported. We examined expression of collagen II (a proliferating chondrocyte marker), CMP (a differentiating chondrocyte marker), and collagen X (a hypertrophic chondrocyte marker). We also examined the expression of the osteoblast markers collagen I and osteopontin. Based on fetal bone *in situ* hybridization results, it appears that there were no differences in the expression of collagen II (Figure 16), CMP (Figure 17), collagen X (Figure 18), collagen I (Figure 19), or osteopontin (Figure 20), when comparing HOM fetuses to their WT littermates. For results where the mRNA signal is

Figure 14. Gross morphology and mineralization of fetal skeleton. Alizarin red S and alcian blue staining was used to compare HOM fetuses to WT littermates. Alizarin red S stains mineralized tissue (such as bone) red whereas alcian blue stains the cartilage blue.

WT HOM

Figure 15. Determination of mineral content of fetal bones. von Kossa's staining was used to compare the amount of mineral present in fetal bone sections of HOM fetuses (B) as compared to WT (A) littermates. Mineralized bone is blackened by silver deposition and osteoid is counterstained with Methyl Green. Pictures shown are bright field images and the various cellular regions of the growth plate are indicated. Normal intensity of staining (black) is seen in HOM fetal femur sections as compared to WT sections. Calibration bars in each panel indicate 50 μm.

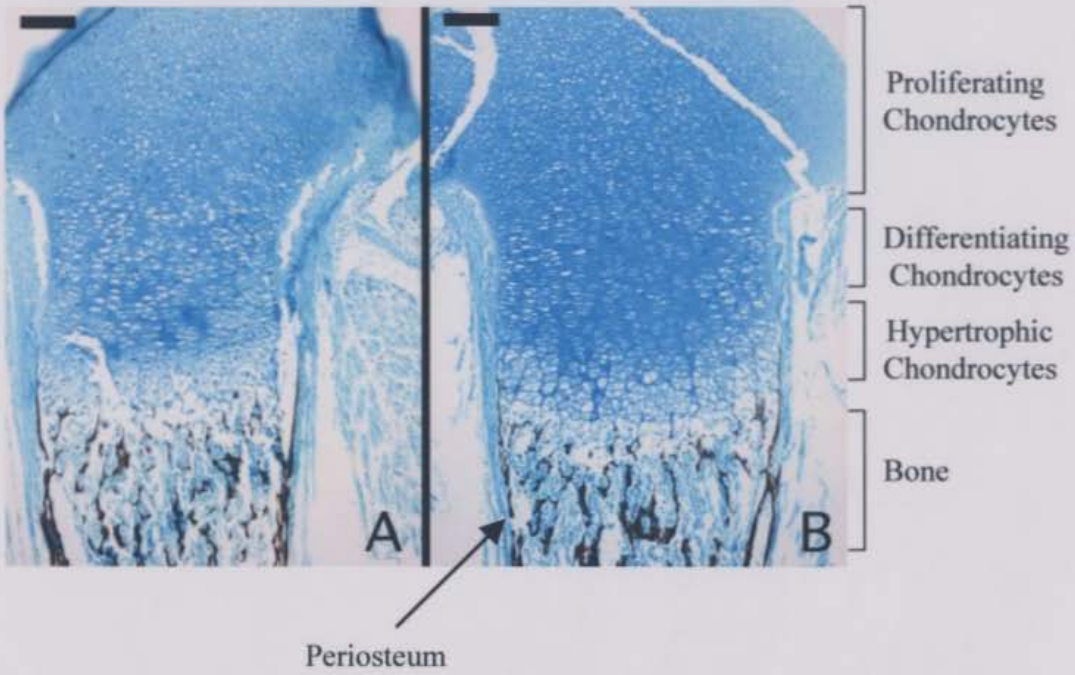
Proliferating
Chondrocytes
Differentiating
Chondrocytes
Hypertrophic
Chondrocytes
Bone
A
B
Periosteum

Table 1: Specificity of mRNAs used for *in situ* hybridization studies on fetal bone tissue sections

Probe	Tissue	Probe Specificity
Collagen I	bone	Osteoblasts
Collagen II	bone	Proliferating chondrocytes
Collagen X	bone	Hypertrophic chondrocytes
Collagenase-3	bone	Osteoblasts
Osteopontin	bone	Osteoblasts
Osteocalcin	bone	Osteoblasts
Cartilage matrix protein	bone	Differentiating chondrocytes
Histone 4	bone	Hypertrophic chondrocytes
Alkaline phosphatase	bone	Osteoblasts
92-kD Gelatinase	bone	Osteoclasts
PTHrP	bone	Proliferating chondrocytes

Figure 16. *In situ* hybridization for Collagen II mRNA in fetal tibia sections. Pictures shown are bright field images of sections counterstained with hematoxylin and eosin. Normal distribution and intensity of Collagen II mRNA signal is seen in HOM fetuses (B) compared to WT littermates (A). The signal (silver grain deposition), which is represented by black, is present throughout the cartilaginous cells of the growth plate. Calibration bars in each panel indicate 50 μm.

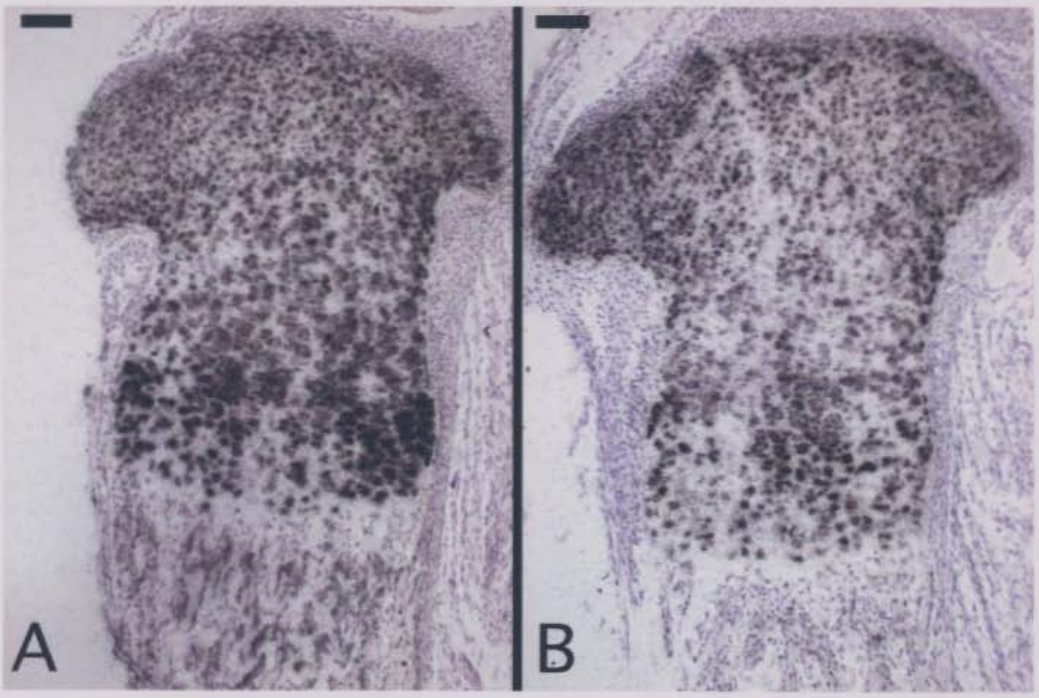
A
B

Figure 17. *In situ* hybridization for cartilage matrix protein (CMP) mRNA in fetal tibia sections. Paired bright field (A and B) and dark field (C and D) images of the same sections (counterstained with hematoxylin and eosin) are shown. Normal distribution and intensity of CMP mRNA signal is seen in HOM fetuses (B and D) compared to WT littermates (A and C). The signal (silver grain deposition), which is represented by black in bright field images and white in dark field images, is present throughout the growth plate and is most intense in the zone of differentiating chondrocytes. Calibration bars in each panel indicate 50 μm.

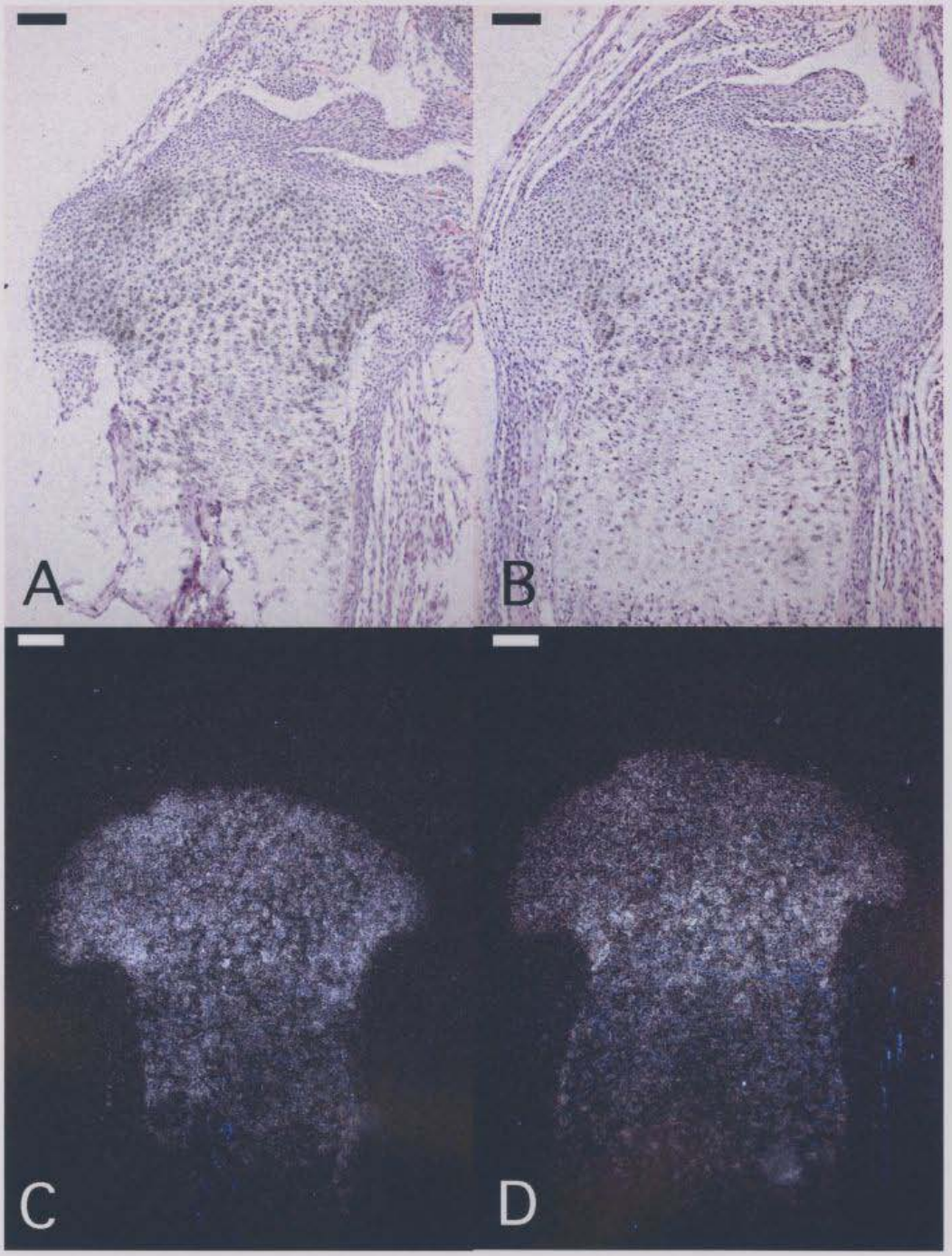
A
B
C
D

Figure 18. *In situ* hybridization for Collagen X mRNA in fetal femur sections. Pictures shown are bright field images of sections counterstained with hematoxylin and eosin. Normal distribution and intensity of Collagen X mRNA signal is seen in HOM fetuses (B) compared to WT littermates (A). The signal (silver grain deposition), represented by black, is intense in the zone of hypertrophic chondrocytes. Calibration bars in each panel indicate 50 μm.

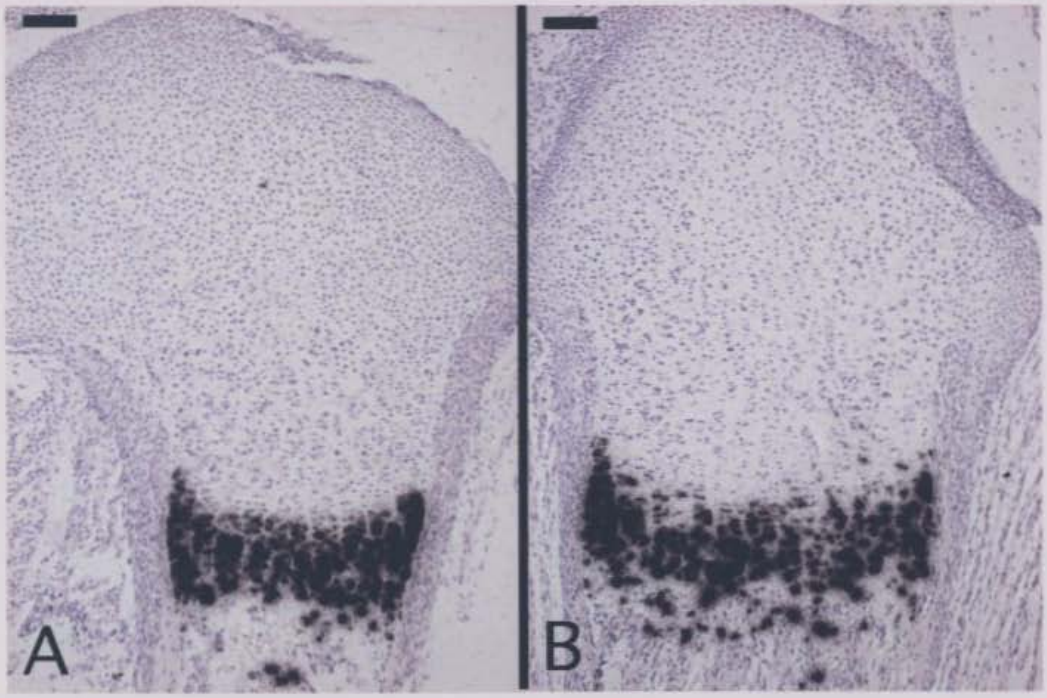
A
B

Figure 19. *In situ* hybridization for Collagen I mRNA in fetal femur sections. Pictures shown are bright field images of sections counterstained with hematoxylin and eosin. Normal distribution and intensity of Collagen I mRNA signal is seen in HOM fetuses (B) compared to WT littermates (A). The signal (silver grain deposition), is present in the periosteum and bone shaft. Calibration bars in each panel indicate 50 μm.

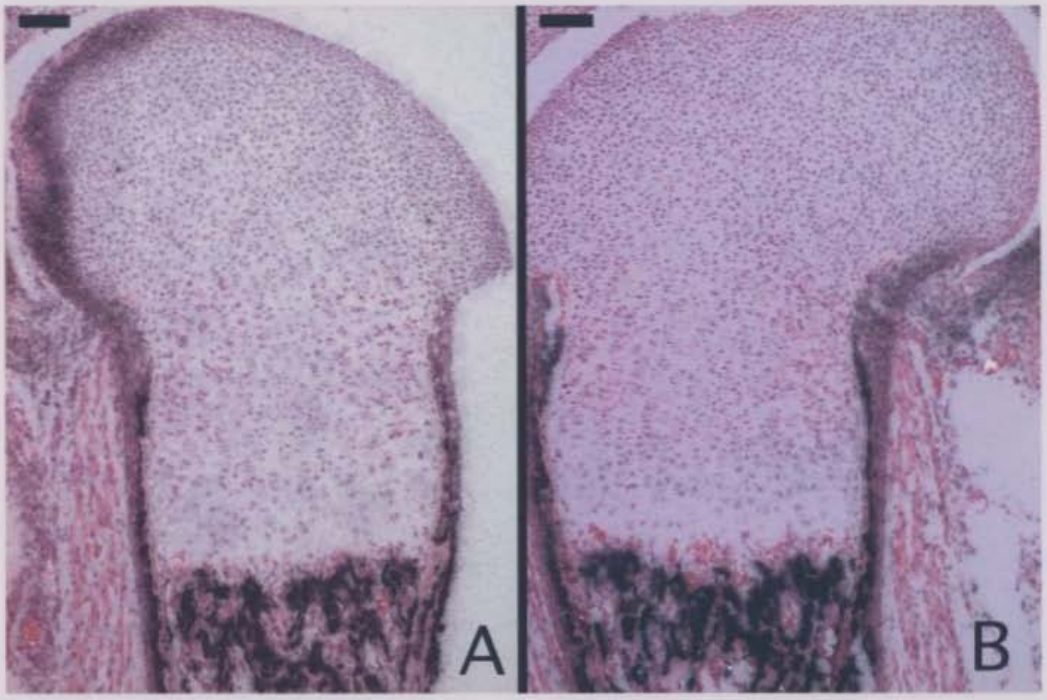
A
B

Figure 20. *In situ* hybridization for osteopontin mRNA in fetal tibia sections. Paired bright field (A and B) and dark field (C and D) images of the same sections (counterstained with hematoxylin and eosin) are shown. Normal distribution and intensity of osteopontin mRNA signal is seen in HOM fetuses (B and D) compared to WT littermates (A and C). The signal (silver grain deposition), which is represented by black in bright field images and white in dark field images, is present in the periosteum and bone shaft. Calibration bars in each panel indicate 50 μm.

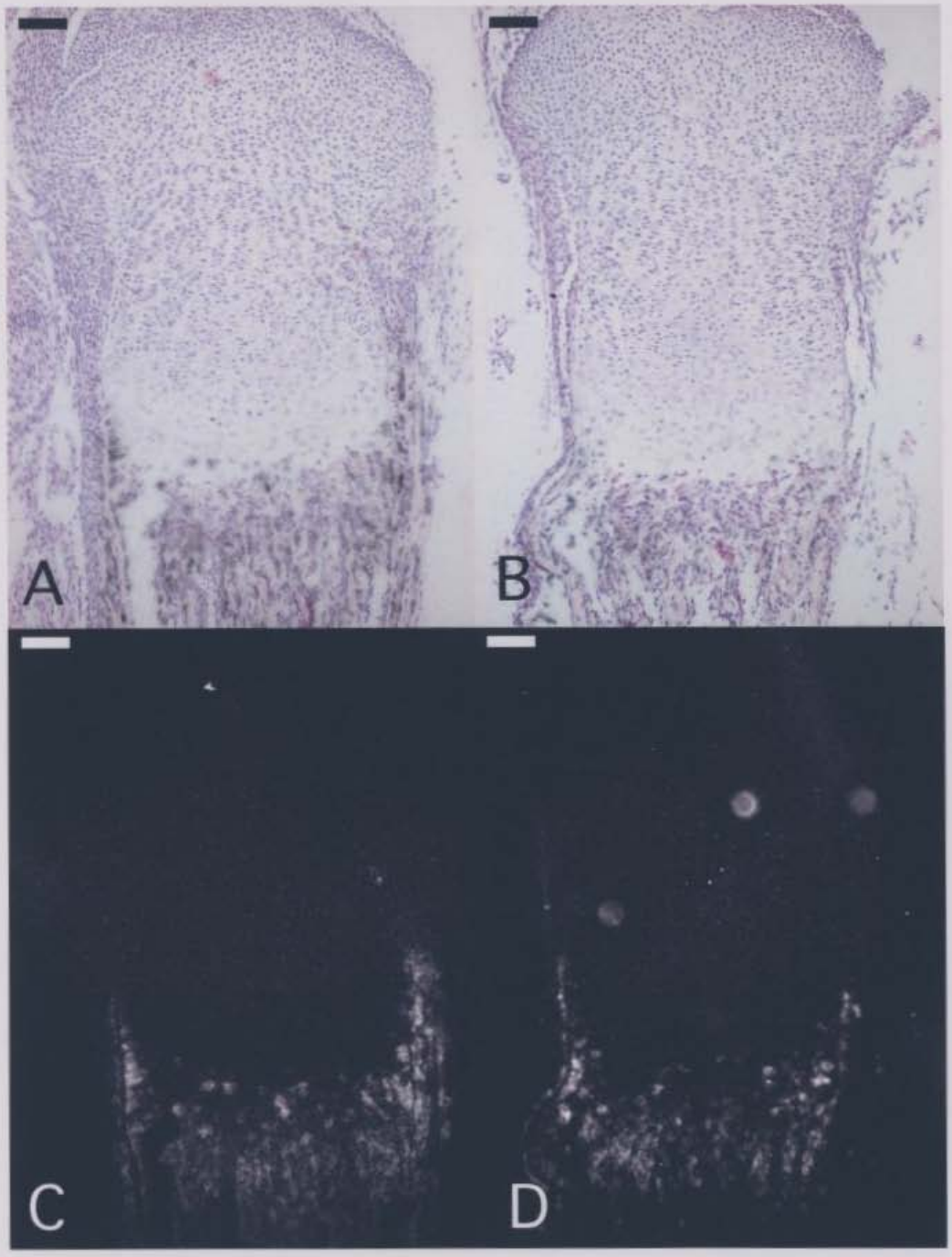
A
B
C
D

intense, only bright field images are shown. However, for those results where the signal is less intense, paired bright field and dark field images are shown. Results of osteoclast markers have not been reported and therefore require further examination.

Based on these results, it appears that loss of fetal CT does not impact the measured parameters of skeletal morphology or development, mineral levels, or gene activity in the growth plate.

3.5 Calciotropic Hormones

We were interested in measuring calciotropic hormones in serum, including those hormones which are known to be important in calcium and bone metabolism, such as PTH, calcitriol, and CT. The purpose of this was to determine whether the loss of CT causes an up-regulation or down-regulation of other hormones. For example, it may be possible that another hormone is compensating for the loss of CT, and that this might be apparent through an increase or decrease in the circulating level of another calciotropic hormone. However, our efforts to measure these hormones were limited by the availability of serum and appropriate assays.

PTH is one of the principal physiological regulators of calcium homeostasis for humans and all terrestrial vertebrates. Therefore, we measured serum PTH levels in fetuses of heterozygous dams using a Rat Intact PTH 1-34 ELISA kit from Immutopics. Serum PTH levels of HOM fetuses (12.60 ± 2.21 pg/ml) did not differ from their HET and WT siblings (12.91 ±1.56 pg/ml and 18.61 ±2.22 pg/ml, respectively; p=0.09) (Figure 21). For several of the WT serum samples the volumes were less than the required 25 µl

Figure 21. Serum PTH levels (mean ± SE) in fetuses of HET dams (ANOVA p=0.09).

The number of observations is indicated in parentheses.

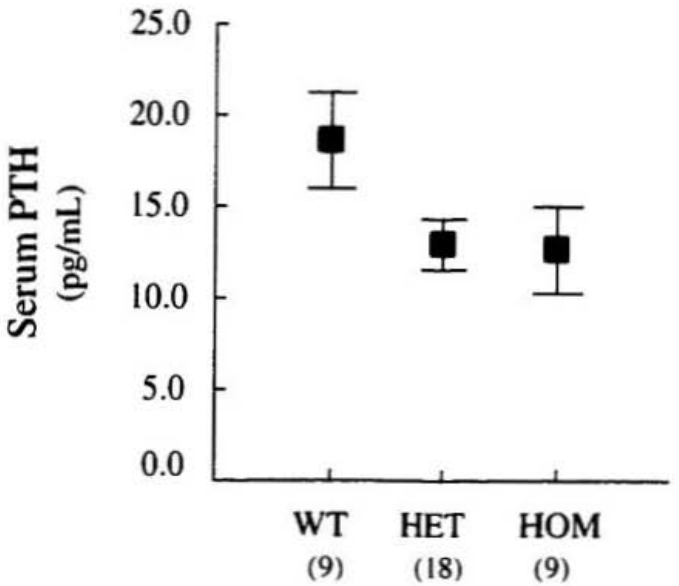
Serum PTH
(pg/mL)
25.0
20.0
15.0
10.0
5.0
0.0
WT
(9)
HET
(18)
HOM
(9)

and were therefore diluted with 0 pg/ml Standard solution. This dilution of the specimens may account for the non-significantly increased PTH levels observed in the WT fetuses.

Serum CT levels were measured in HET and HOM dams and in their fetuses using a Rat CT IRMA Kit from Immutopics. HET dams had a mean serum CT level of 95.02 ±10.30 pg/ml as compared to 7.16 ±16.82 pg/ml in HOM dams (p=0.0016) (Figure 22). Assuming that CT is not present in HOM dams, the value of 7.16 pg/ml must represent a true zero and the threshold of detectability for CT in mice. The stated assay sensitivity is 0.6 pg/ml with this kit in rats. However, the threshold of sensitivity has not been determined in mice.

Fetal serum CT analysis revealed a step-wise dose dependent response by genotype in fetuses of HET dams (WT: 125.62 ±16.11 pg/ml > HET: 48.86 ±12.30 pg/ml > HOM: 7.37 ±14.21 pg/ml; p=0.00004) (Figure 23A). Similar results were found in fetuses of HOM dams (HET: 41.11 ±5.98 pg/ml > HOM: 9.42 ±3.71 pg/ml; p=0.0004) (Figure 23B). The CT levels of HET and HOM fetuses respectively do not vary by the mothers genotype (Figure 23). This is consistent with the hypothesis that CT does not cross the placenta. Furthermore, the CT levels of HOM dams and HOM fetuses are all identical. This is consistent with the hypothesis that the level of ~8 pg/mL represents a true zero for this assay in mouse serum.

3.6 Molecular Mechanisms of Placental Calcium Transport

Placentas were studied in order to determine what compensatory effects on cellular morphology may occur as a consequence of the loss of CT. Thus, such elements

Figure 22. Serum CT levels (mean ± SE) in HET and HOM dams (p=0.0016). The number of observations is indicated in parentheses.

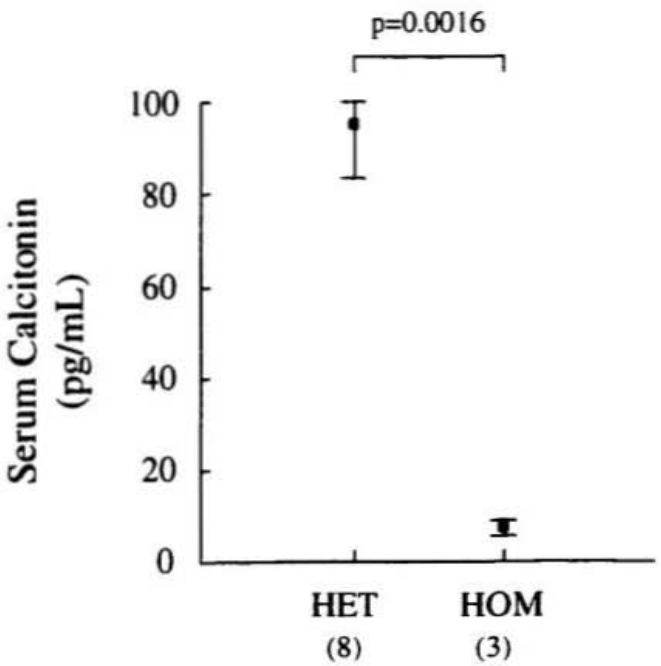
p=0.0016
Serum Calcitonin
(pg/mL)
100
80
60
40
20
0
HET
(8)
HOM
(3)

Figure 23. Serum CT levels (mean ± SE) in fetuses of HET (A) and HOM (B) dams. A step-wise decrease is seen, according to genotype, in fetuses of both HET and HOM dams. HET fetal CT levels are the same between HET and HOM dams and HOM fetal CT levels are the same between HET and HOM dams. The number of observations is indicated in parentheses.

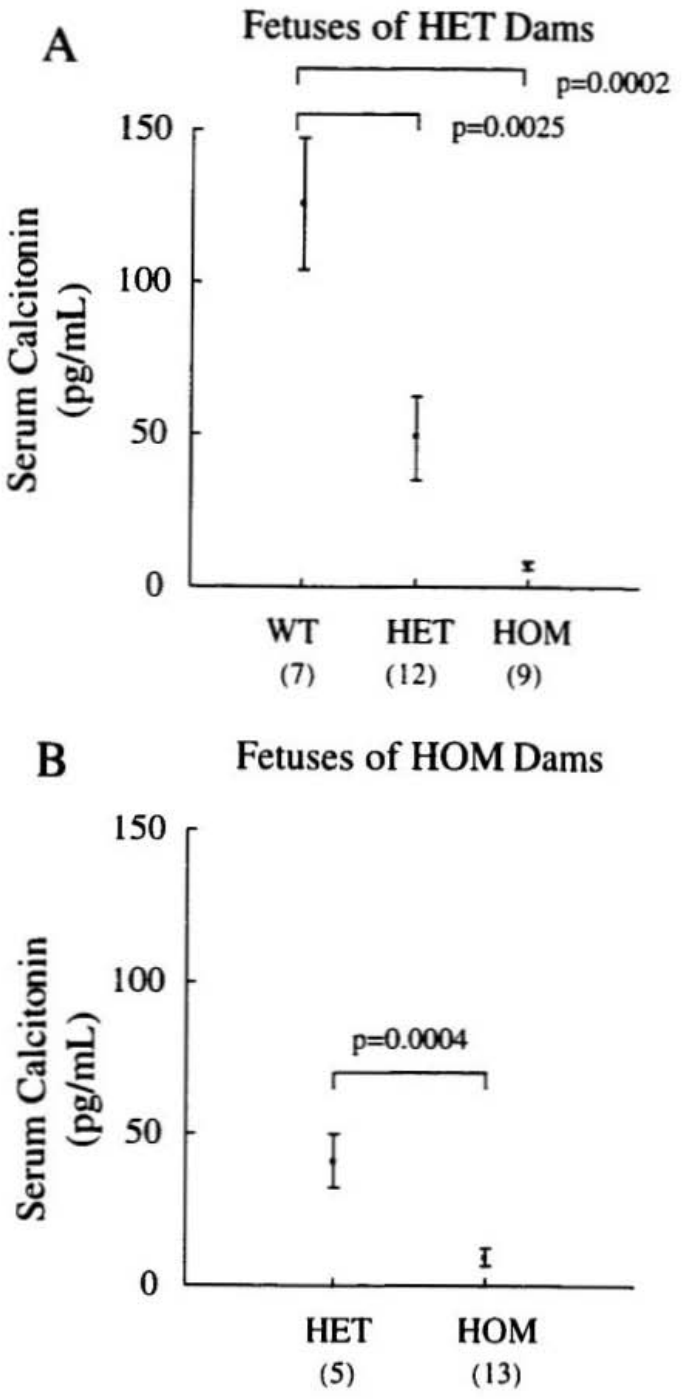
A
Fetuses of HET Dams
p=0.0002
p=0.0025
150
100
50
0
Serum Calcitonin
(pg/mL)
WT
HET
HOM
(7)
(12)
(9)
B
Fetuses of HOM Dams
150
100
50
0
Serum Calcitonin
(pg/mL)
p=0.0004
HET
HOM
(5)
(13)

as the size, appearance and distribution of trophoblasts as well as the presence of the IPYS were examined. Since the placenta is the site of calcium transfer, it was also important to determine whether the cells and factors they express, which are involved in this transfer, are altered in CT gene-deleted mice. The site of active transport is likely to be in the trophoblast cells and in the endoderm of the IPYS in rodents. These cells are in closest proximity to the maternal circulation and the IPYS cells express particularly high levels of Ca^{++} ATPase (the "calcium pump") and high levels of calbindin-D_{9k} (a calcium-binding protein). Calbindin-D_{9k} is also known to be an IPYS marker. Therefore, we examined the level of expression of calbindin-D_{9k} and Ca^{++} ATPase in placentas of CT gene-deleted fetuses compared to their WT siblings. Based on placental *in situ* hybridization results it appears that there are no differences in the intensity or location of mRNA expression of calbindin-D_{9k} (Figure 24) and Ca^{++} ATPase (Figure 25), nor did there appear to be any gross differences in cellular appearance or structure. In addition, a preliminary study on placental weights of fetuses of HET dams suggests that there are no differences among fetuses (0.0736 ±0.0089 g in HOM fetuses (n=2), 0.0838 ±0.0052 g in HET fetuses (n=6), and 0.0917 ±0.0052 g in WT fetuses (n=6); p=0.24).

3.7 Calcitonin and the Calcitonin-Receptor in the Placenta

Contradictory evidence exists on whether or not the CT and CT-receptor genes are actually expressed in the placenta. Furthermore, if CT and its receptor are not normally present in the placenta, that could explain why we see little effect upon loss of the CT gene. The CT knockout placenta represents an ideal model to determine the specificity of

Figure 24. *In situ* hybridization for calbindin-D_{9k} mRNA expression in 5 μm placental sections. Pictures shown are bright field images of sections counterstained with hematoxylin and eosin. Normal distribution and intensity of calbindin-D_{9k} mRNA signal is seen in HOM fetuses (B) compared to WT littermates (A). Intense signal (silver grain deposition), which is represented by black, is seen in the IPYS and light signal is seen in trophoblasts. The appearance and distribution of trophoblasts and IPYS also appear to be normal in HOM fetuses. Calibration bars in each panel indicate 50 μm.

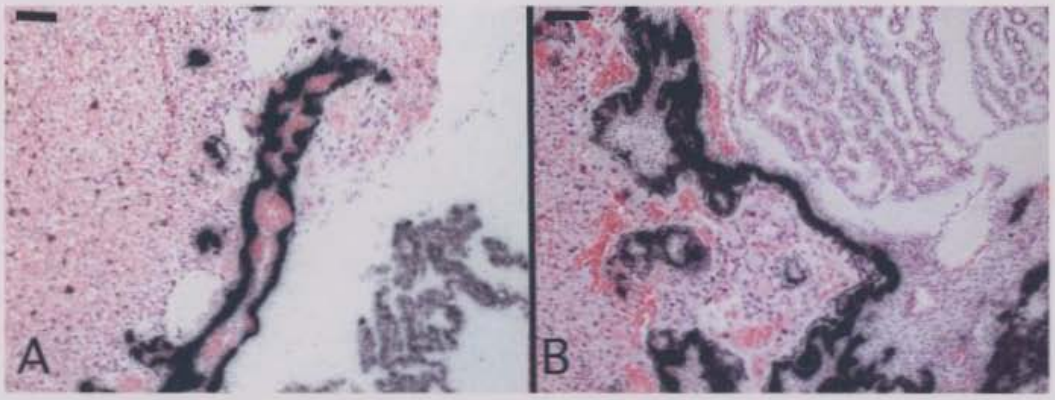
A
B

Figure 25. *In situ* hybridization for Ca^{++}ATPase mRNA expression in 5 μm placental sections. Pictures shown are bright field images of sections counterstained with hematoxylin and eosin. Normal distribution and intensity of Ca^{++}ATPase mRNA signal is seen in HOM fetuses (B) compared to WT littermates (A). Intense signal, (silver grain deposition) which is represented by black, is seen in the IPYS and less intense signal is seen in trophoblasts. The appearance and distribution of trophoblasts and IPYS also appear to be normal in HOM fetuses. Calibration bars in each panel indicate 50 μm.

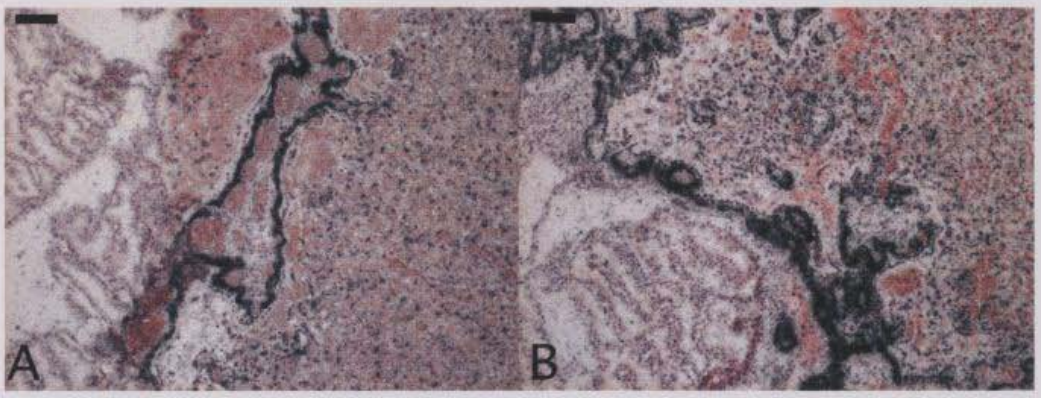
A
B

CT mRNA and immune signals, and determine if it is truly present or not. Therefore, *in situ* hybridization and immunohistochemistry were performed to determine if these genes are expressed in placental tissue and where they are expressed. CT mRNA was diffusely expressed throughout the WT placenta, in the intraplacental yolk sac and in the labyrinthine trophoblasts (Figure 26). A signal was not detected in the extra placental yolk sac (EPYS). In contrast, CT mRNA was not detected in HOM placentas, thereby confirming the specificity of the signal detected in the WT placenta. Similar results were found by immunohistochemistry, using a CT antibody (Figure 27). Antibody to CT-receptor revealed moderate, diffuse staining in the IPYS and labyrinthine trophoblasts (Figure 28). The most intense staining was seen in the EPYS.

These results provide evidence that CT and the CT-receptor are indeed present in the placenta. Being located in the placenta, CT would be expected to play some role in placental function.

Figure 26. *In situ* hybridization for CT mRNA expression in 5 μm placental sections. Paired bright field (A and C) and dark field (B and D) images of the same sections (counterstained with hematoxylin and eosin) are shown. CT mRNA signal is present throughout labyrinthine trophoblasts (T) and both layers of the IPYS (arrows) in WT placental sections (A and B). There is no signal detected in the EPYS (E). Corresponding images from HOM placental sections (C and D) show no signal. The signal (silver grain deposition) is represented by black in bright field images and white in dark field images. Calibration bars in each panel indicate 50 μm.

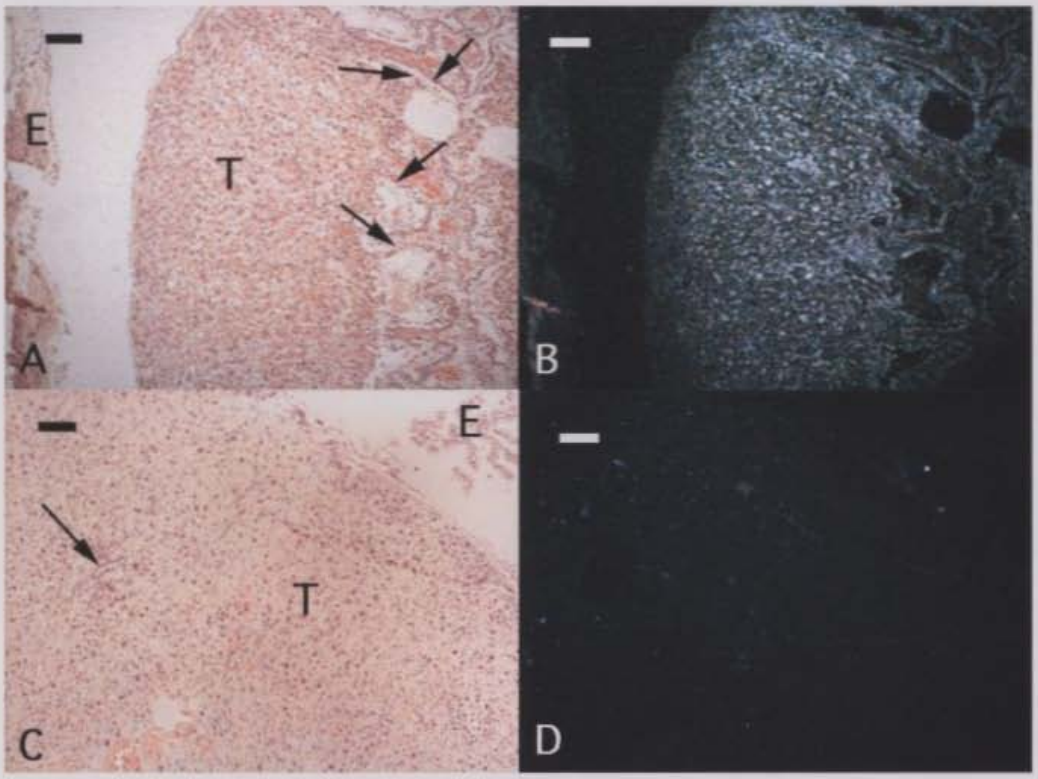
E
T
A
B
E
T
C
D

Figure 27. Placental immunohistochemistry using CT primary antibody. CT immunoreactivity is present in the IPYS in WT (A) as compared to HOM placenta (B). Bright field images are shown and the calibration bar in each panel indicates 50 μm. Arrows indicate IPYS.

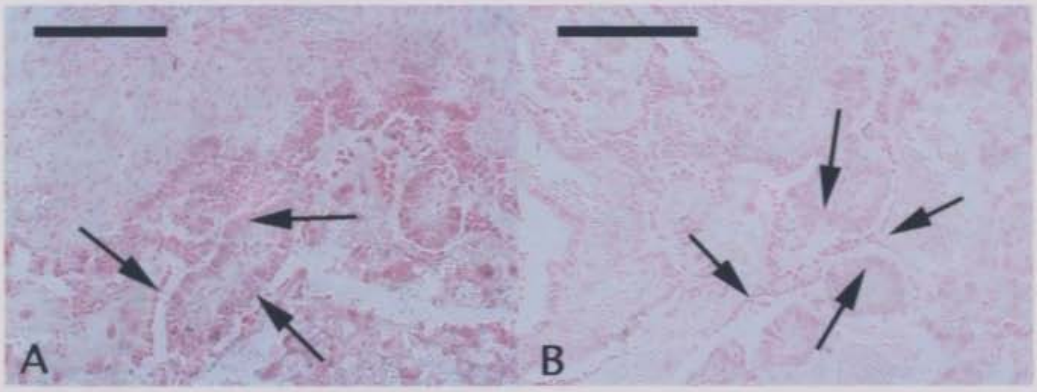
A
B

Figure 28. Immunohistochemistry using CT-receptor primary antibody on WT placental sections (B). The adjacent control section (A) received identical treatment to the experimental sections except for the use of the primary antibody. CT-receptor immunoreactivity is present at low levels throughout the labyrinthine trophoblasts (T) and the IPYS (arrows), and at more intense levels in the EPYS (E). Bright field images are shown and the calibration bar in each panel indicates 50 μm. Arrows indicate IPYS.

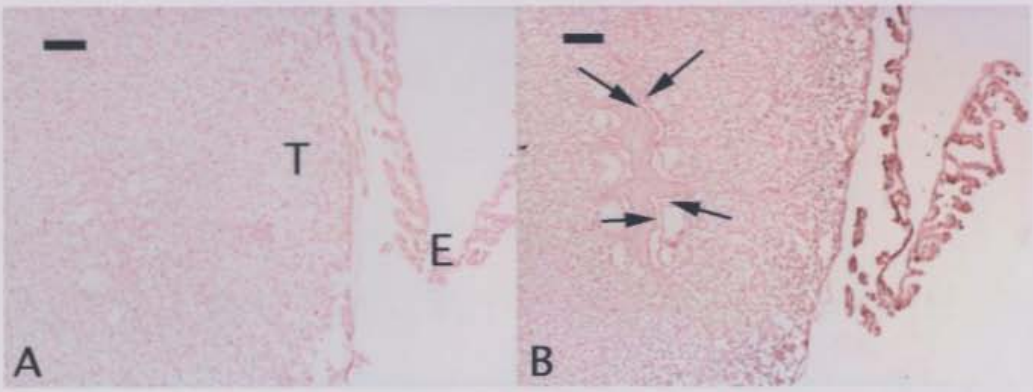
T
E
A
B

IV DISCUSSION

In these studies we measured several parameters of calcium and bone metabolism to determine whether the loss of the CT gene affected the fetal-placental unit. In this way, we expected to determine whether CT was critically required for any aspect of normal fetal-placental calcium homeostasis and skeletal development. We examined the maternal effects of CT deletion, placental calcium transport, as well as aspects of fetal mineral physiology and skeletal development. We also looked at the molecular mechanisms involved in placental calcium transport, assayed calciotropic hormones, and examined the presence of CT and its receptor in the placenta. We have demonstrated that homozygous deletion of the CT gene did eliminate CT but did not affect maternal or fetal ionized calcium levels, the rate of fetal-placental calcium transfer, serum phosphorus levels, or the amount of mineral present in each fetal skeleton. It also did not affect fetal serum PTH levels, the gross skeletal morphology, the expression of important bone markers, or calbindin-D_{9K} or Ca^{++} ATPase expression in placental tissue. However, we did find that maternal loss of CT resulted in a reduction in litter size and that maternal and fetal loss of CT resulted in a reduction in the concentration of magnesium in the fetal circulation and possibly in the fetal skeleton. It is important to point out that since a CT/CGRP knockout model was actually studied, the results demonstrate that lack of both hormones had little effect. In addition, our studies confirm that the genes for CT and the CT-receptor are located in the murine placenta, although the function of CT and its

receptor in the placenta is unclear since no abnormality of placental structure or function has been demonstrated.

Early in the study we noticed that HOM dams often had smaller litters than their HET siblings. We confirmed that HOM dams had significantly smaller *in utero* litter sizes than HET dams. Our data clearly show that CT deficiency will result in a lower litter size, but cannot distinguish whether this is due to an impairment in oocyte number, oocyte release, fertilization, implantation, or survival through early embryonic development to the fetal stage. However, we do know that since we did not see a selective reduction in the number of HOM fetuses, that it is the loss of maternal CT that is affecting the litter size. Our finding is not without precedent. CT has been shown to be involved in the implantation of the mammalian embryo to the uterine wall. Zhu and others (40) found that the administration of antisense CT oligodeoxynucleotides into the lumen of the preimplantation rat uterus resulted in a severe impairment in embryonic implantation. They therefore proposed that CT plays a crucial role in the uterus during blastocyst implantation. In addition, it was demonstrated that CT expression in the human endometrium is temporarily restricted to the mid-secretory phase of the cycle, which closely overlaps with the putative window of implantation (41). Thus, one possible interpretation of our findings is that a loss of CT reduces the likelihood of implantation of the embryo to the uterus, resulting in fewer embryos actually succeeding in implantation. Although reduced implantation may be a factor, further study is needed in order to rule out the effects of the lack of CT on other stages of development, from oocyte onward, as previously mentioned.

The notion that CT might play a role in magnesium regulation appears to be a novel finding. However, since calcium, phosphorus, and magnesium regulation are inter-related, it is not that surprising a result. It is possible that CT may influence the transport of magnesium across the placenta from the mother to the fetus; unfortunately, an appropriate magnesium isotope (affordable and with a sufficiently long half-life) to use to study this possibility is not available. In order to determine how CT affects magnesium, it would be relevant to study the effects of CT on magnesium handling by the fetal kidney, which could be studied indirectly by measuring the magnesium content in amniotic fluid. Amniotic fluid is largely composed of fetal urine and is accepted to be an indirect measure of renal function. For example, if there is less magnesium crossing the placenta to the fetus we would expect to see a decrease in the magnesium content of the amniotic fluid. Whereas if the fetal kidneys are actually wasting magnesium, we would expect to see an increase in the magnesium content of the in the amniotic fluid. Another possibility is that CT is influencing another factor which in turn is affecting magnesium regulation. One method to confirm that CT is directly involved in magnesium homeostasis would be to treat HOM fetuses with CT *in utero* to see if magnesium levels (in serum and bone) return to normal.

Based on the measured parameters, it appears that CT gene-deletion does not affect the skeletal morphology, net mineral accretion, or gene activity in the growth plate. However, some of these methods are semi-quantitative and there may be differences that we are unable to detect using such methods. For example, we looked at gene expression but did not examine cell size, number or detailed microscopic appearance. It is also

possible that other markers which we have not studied might show differences. In addition, precise measurements of fetal bones should be taken to determine how the loss of CT affects bone structure and size. It is very important that such studies be done since it is possible that we are overlooking small details or differences between the fetal skeletons.

Our results confirm that CT has indeed been ablated in the knockout mice. The results revealed a step-wise decrease in CT levels by genotype with WT having the highest level of CT, HOM having no CT, and HET having an intermediate level. This indicates that one copy of the CT gene is not sufficient to ensure normal levels of CT. Similar intermediate effects of a HET state have previously been reported in *Hoxa3* knockout mice (these mice lack parathyroid glands) whereby PTH levels revealed a dosing effect according to genotype (7). The results also support previous findings that CT does not cross the placenta (26) since HOM fetuses had the same low level of CT regardless of whether the dam produced CT (HET dam) or not (HOM dam). However, the kit that was used for the CT assay was designed for detection of CT in rats, not mice. We found HOM fetal and maternal CT results to be in the range of approximately 8 pg/ml. This is most likely the threshold of detection for CT in mice (using this kit), confirming that CT is not present in the HOM mice (adults and fetuses). On the other hand, if this value is not a true zero, then it would have to be explained how HOM mice have low levels of CT present in serum. For example, is CT being transferred from HET fetuses to HOM dams and from there to HOM fetuses *in utero*, thereby accounting for similarly low levels of CT in HOM fetuses and dams? This could be tested by HOM x

HOM matings which would produce only HOM fetuses and eliminate any possible fetal→ maternal→ fetal CT transfer. Another possibility is that there could be another gene which produces CT, however this is highly unlikely given that the mouse genome has been fully sequenced and no CT homologous genes have been reported.

We were interested in examining other calciotropic hormones known to be involved in calcium in bone homeostasis. Despite the fact that loss of CT did not significantly affect fetal serum PTH levels, it may still be that some other hormone is compensating for the loss of CT. Therefore, further measurements of hormones such as PTHrP, calcitriol, and sex steroids such as estrogen in the knockout mice would be an asset to the study. These hormones have not yet been measured simply due to the limiting factor of the availability of sufficient fetal serum.

Placental *in situ* hybridization results imply that there are no differences in the intensity or location of expression of calbindin-D_{9K} and Ca^{++} ATPase in HOM placentas and that the cellular and structural appearance of the placentas also appear to be normal. However, there are still aspects which could be looked at in more detail, since our observations are more qualitative. For example, although preliminary results suggest that there are no placental weight differences among fetuses of HET dams, a larger investigation is required. In addition, an in depth examination of the size and number of trophoblasts in placental tissue, as well as measurements of the volume of IPYS in placental tissue could be taken. The expression of other important placental markers could also be examined.

Identifying the location of calciotropic genes in the placenta, will help determine the pathway involved in placental calcium transport and provide insight into which genes are involved in the process. The localization of expression of many calciotropic genes has either not been reported or many of these reports used outdated methods or antibodies whose specificity would not be considered adequate by modern standards. Contradictory evidence has existed on whether or not the CT gene is expressed in the placenta. For example, it had been reported that CT is expressed in the rat and human placenta (42) (43). However, these results are inconclusive partly due to problems with antibody specificity and the studies did not identify the specific cells that appeared to secrete CT. In contrast, several studies have demonstrated the presence of the CT-receptor in the placenta. For example, using radiolabeled–CT binding studies, the CT-receptor was found to be located in the syncytiotrophoblast brush border (facing the mother) as well as in the basal plasma membrane (facing the fetus) of the human placenta (44). Our studies show that CT and the CT-receptor are present in the labyrinthine trophoblasts and IPYS of the placenta.

We examined several indices of calcium and bone metabolism in this study. It appears that the complete loss of either maternal or fetal CT did not affect the majority of these parameters. However, the results do imply that there is a relationship between the loss of CT and magnesium regulation. They also support previous findings that CT is involved in the implantation of the mammalian embryo to the uterine wall. Taken as a whole, these results suggest that CT is not essential for the survival and development of the fetus nor for any parameter of calcium metabolism that we have measured thus far.

Such negative results are consistent with the theory that CT is a vestigial hormone in mammals that has no physiological role in calcium homeostasis.

V. REFERENCE LIST

1. Strewler, G.J. 1997. Mineral Metabolism and Metabolic Bone Disease. In Basic and Clinical Endocrinology. F.S. Greenspan and Strewler, G.J., editors. Stamford, CT: Appleton & Lange. 263-316.

2. Bringhurst, F.R., Demay, M.B., and Kronenburg, H.M. 1998. Hormones and Disorders of Mineral Metabolism. In Williams Textbook of Endocrinology. J.D. Wilson, Foster, D.W., Kronenburg, H.M., and Larson, P.R., editors. Philadelphia,PA: W.B. Saunders Company. 1155-1209.

3. Broadus, A.E. 1999. Mineral Balance and Homestasis. In Primer on the Metabolic Bone Diseases and Disorders of Mineral Metabolism. M.J. Favus, editor. Philadelphia, PA: Lippencott Williams & Wilkins. 74-80.

4. Holick, M.F. 1999. Vitamin D: Photobiology, Metabolism, Mechanism of Action, and Clinical Applications. In Primer on the Metabolic Bone Diseases and Disorders of Mineral Metabolism. M.J. Favus, editor. Philadelphia, PA: Lippencott Williams & Wilkins. 92-98.

5. Kovacs, C.S. 2000. Exploring the normal regulation of fetal-placental calcium metabolism through the use of targeted gene ablation in fetal mice. *Drug Development Research* 49:167-173.

6. Kovacs, C.S. and Kronenberg, H.M. 1997. Maternal-fetal calcium and bone metabolism during pregnancy, puerperium and lactation. *Endocrine Reviews* 18:832-872.

7. Kovacs, C.S., Manley, N.R., Moseley, J.M., Martin, T.J., and Kronenberg, H.M. 2001. Fetal parathyroids are not required to maintain placental calcium transport. *Journal of Clinical Investigation* 107:1007-1015.

8. Kovacs, C.S., Chafe, L.L., Fudge, N.J., Friel, J.K., and Manley, N.R. 2001. Parathyroid hormone regulates fetal blood calcium and skeletal mineralization independently of PTHrP. *Endocrinology* 142:In Press.

9. Kovacs, C.S., Lanske, B., Hunzelman, J.L., Guo, J., Karaplis, A.C., and Kronenberg, H.M. 1996. Parathyroid hormone-related peptide (PTHrP) regulates fetal-placental calcium transport through a receptor distinct from the PTH/PTHrP receptor. *Proceedings of the National Academy of Sciences, U.S.A.* 93:15233-15238.

10. Kovacs, C.S., Ho-Pao, C.L., Hunzelman, J.L., Lanske, B., Fox, J., Seidman, J.G., Seidman, C.E., and Kronenberg, H.M. 1998. Regulation of murine fetal-placental calcium metabolism by the calcium-sensing receptor. *J.Clin.Invest.* 101:2812-2820.

11. Copp, D.H., Cameron, E.C., Cheney, B.A., Davidson, A.G., and Henze, K.G. 1962. Evidence for Calcitonin-A New Hormone from the Parathyroid That Lowers Blood

Calcium. *Endocrinology* 70:638-649.

12. Foster, G.V., Baghdiantz, A., Kumar, M.A., Slack, E., Soliman, H.A., and MacIntyre, I. 1964. Throid origin of calcitonin. *Nature* 202:1303-1305.

13. Pearse, A.G.E. and Cavalheira, A.F. 1967. Cytochemical evidence for an ultimobranchial origin of rodent thyroid C cells. *Nature* 214:929-930.

14. Macintyre, I. 1995. Calcitonin: Physiology, Biosynthesis, Secretion, Metabolism, and Mode of Action. In Endocrinology. L.J. DeGroot, editor. Philadelphia: W.B. Saunders. 978-989.

15. Azria, M. 1989. The Calcitonins. Karger, Switzerland.

16. Copp, D.H. 1994. Calcitonin: discovery, development, and clinical application. *Clinical and Investigative Medicine* 17:268-277.

17. Deftos, L.J., Roos, B.A., and Oates, E.L. 1999. Calcitonin. In Primer on the Metabolic Bone Diseases and Disorders of Mineral Metabolism. M.J. Favus, editor. Philadelphia, PA: Lippencott Williams & Wilkens. 99-104.

18. Martin, T.J., Findlay, D.M., Moseley, J.M., and Sexton, P.M. 1998. Calcitonin. In Metabolic Bone Disease. L.V. Avioli and Krane, S.M., editors. San Diego, CA:

Academic Press. 95-121.

19. Swaminathan, R., Bates, R.F.L., and Care, A.D. 1972. Fresh evidence for the physiological role of calcitonin in calcium homeostasis. *Journal of Endocrinology* 53:xlvi-xlvii.

20. Swaminathan, R., Bates, R.F.L., Bloom, S.R., Ganguli, P.C., and Care, A.D. 1973. The relationship between food, gastro-intestinal hormones and calcitonin secretion. *Journal of Endocrinology* 59:217-230.

21. Taylor, T.G., Lewis, P.E., and Balderstone, O. 1975. Role of calcitonin in protecting the skeleton during pregnancy and lactation. *The Journal of Endocrinology* 66:297-298.

22. Barlet, J.P. 1974. Role physiologique de la calcitonine chez la chèvre gestante ou allaitante. *Annales De Biologie Animale, Biochimie, Biophysiques.* 14:447-457.

23. Barlet, J.P. and Garel, J.M. 1975. Physiological role of calcitonin in pregnant goats and ewes. In Calcium regulating hormones: Proceedings of the fifth parathyroid conference, Oxford, United Kingdom, July 21-26, 1974. R.V. Talmage, Owen, M., and Parsons, A., editors. Amsterdam: Excerpta Medica. 119-121.

24. Leroyer-Alizon, E., David, L., and Dubois, P.M. 1980. Evidence for calcitonin in

the thyroid gland of normal and anencephalic human fetuses: immunological localization, radioiummunoassay, and gel filtration of thyroid extracts. *Journal of Clinical Endocrinology and Metabolism* 50:316-321.

25. Garel, J.M., Care, A.D., and Barlet, J.P. 1974. A radioimmunoassay for ovine calcitonin: an evaluation of calcitonin secretion during gestation, lactation and foetal life. *J.Endocrinol.* 62:497-509.

26. Garel, J.M., Milhaud, G., and Sizonenko, P. 1969. [Thyrocalcitonin and the placental barrier in rats]. *Comptes Rendus Hebdomadaires Des Seances De L'Academie Des Sciences* 269:1785-1787.

27. Garel, J.M. and Barlet, J.P. 1978. Calcitonin in the mother, fetus and newborn. *Annales De Biologie Animale, Biochimie, Biophysique* 18:53-68.

28. Barlet, J.P. 1985. Calcitonin may modulate placental transfer of calcium in ewes. *Journal of Endocrinology* 104:17-21.

29. Barlet, J.P., Davicco, M.J., and Coxam, V. 1992. Calcitonin modulates parathyroid hormone related peptide-stimilated calcium placental transfer. In Calcium regulating hormones and bone metabolism. D.V. Cohn and Gennari, C., editors. Amsterdam: Elsevier Science Publishers. 124-128.

30. Care, A.D., Caple, I.W., Abbas, S.K., and Pickard, D.W. 1986. The effect of fetal thyroparathyroidectomy on the transport of calcium across the ovine placenta to the fetus. *Placenta.* 7:417-424.

31. Karsenty, G. 2001. Chondrogenesis just ain't what it used to be. *The Journal of Clinical Investigation* 107:405-407.

32. 1992. Miller-Keane Encyclopedia & Dictionary of Medicine, Nursing, & Allied Health. W.B. Saunders Company, Philadelphia.

33. Steven, D.H. 1975. Anatomy of the Placental Barrier. In Comparative Placentation. D.H. Steven, editor. New York: Academic Press, Inc. 25-27.

34. Ramsey, E.M. 1982. The Placenta: Human and Animal. Praeger, New York.

35. Kovacs, C.S., Chafe, L.L., Woodland, M.L., McDonald, K.R., Wookey, P., and Kronenberg, H.M. 2001. Calcitropic gene expression in the murine placenta suggests a role of the intraplacental yolk sac in maternal-fetal calcium exchange. *Submitted to the American Journal of Physiology.*

36. Ogura, Y., Takakura, N., Yoshida, H., and Nishikawa, S. 1998. Essential Role of Platelet-Derived Growth Factor Receptor α in the Development of the Intraplcental Yolk Sac/Sinus of Duval in Mouse Placenta. *Biology of Reproduction* 58:65-72.

37. Hoffe, A.O., Thomas, P.M., Cote, G.J., Qiu, H., Bain, S., Puerner, D., Serachan, M., Loyer, E., Pinero, G., Ordonez, N. *et al.* 1998. Generation of a calcitonin knockout mouse model. *Journal of Bone and Mineral Research* 23 (suppl 5): (Abstr.)

38. Bills, C.E., Eisenberg, H., and Pallante, S.L. 1971. Complexes of organic acids with calcium phosphate: the von Kossa stain as a clue to the composition of bone mineral. *Johns Hopkins Medical Journal* 128:194-207.

39. Pearse, A.G.E. 1985. Histochemistry: Theoretical and Applied. Churchill Livingstone, New York.

40. Zhu, L.J., Bagchi, M.K., and Bagchi, I.C. 1998. Attenuation of Calcitonin Gene Expression in Pregnant Rat Uterus Leads to a Block in Embryonic Implantation. *Endocrinology* 139:330-339 (Abstr.)

41. Kumar, S., Zhu, L.J., Polihronis, M., Cameron, S.T., Baird. D.T., Schatz, F., Dua, A., Ying, Y.K.B.M.K., and Bagchi, I.C. 1998. Progesterone induces calcitonin gene expression in human endometrium within the putative window of implantation. *Journal of Clinical Endocrinology and Metabolism* 83:4443-4450.

42. Jousset, V., Legendre, B., Besnard, P., Segond, N., Jullienne, A., and Garel, J.M. 1988. Calcitonin-like immunoreactivity and calcitonin gene expression in the placenta and in the mammary gland of the rat. *Acta Endocrinologica* 119:443-51.

43. Balabanova, S., Kruse, B., and Wolf, A.S. 1987. Calcitonin secretion by human placental tissue. *Acta Obstetricia et Gynecologica Scandinavica* 66:323-326.

44. Lafond, J., Simoneau, L., Savard, R., and Lajeunesse, D. 1994. Calcitonin receptor in human placental syncytiotrophoblast brush border and basal plasma membranes. *Molecular and Cellular Endocrinology* 99:285-92.

DNA EXTRACTION FROM TISSUES

1. Put tissue (e.g. tail tip) in Eppendorf tubes containing 0.5 ml lysis buffer. Buffer is stored at room temperature; proteinase K is added shortly before use.

2. Incubate overnight at 55 °C on shaker.

3. Next morning, shake horizontally by hand for 2 to 3 minutes, and spin on micro centrifuge for 10 minutes at maximum speed to precipitate hair (not necessary for fetal samples!).

4. Pour supernatant into fresh Eppendorf tubes containing 0.5 ml isopropanol, and invert to precipitate DNA.

5. Pick DNA up with small pipette tips and put it into Eppendorf tubes containing 0.5 ml water.

6. Shake by hand for 5 minutes to dissolve DNA into a viscous solution.

7. Add 0.5 ml of phenol/chloroform/isoamyl alcohol (100:100:1) and shake vigorously for approx. 1 min. A turbid, milky solution should result.

8. Spin 2 minutes at maximum speed in micro centrifuge.

9. Carefully aspirate the supernatant and place it in fresh Eppendorf tubes. Add 1 ml of 25:1 EtOH:NaOAc solution. Invert several times until DNA comes out of solution.

10. Spin for 10 minutes at maximum speed to precipitate DNA. A tiny pellet should be seen.

11. Discard the supernatant by pouring it off, then add 1 ml of 70% EtOH.

12. Pour off the EtOH and dry the pellet by leaving the Eppendorf tube inverted, or place it in a vacuum centrifuge (Speed-Vac).

13. Resuspend DNA pellet in 50 µL TE (Tris-EDTA) and put in warm water bath for at least 20 minutes to resuspend. A viscous solution should result. Add more TE if too viscous.

14. Allow the DNA to go into solution overnight before using (can be used within 20 min for PCR). Store at 4 °C.

PERFUSION OF ADULT MICE

1. Fill a 20 ml syringe with PBS and another with 4% PFA (paraformaldehyde) or 10% formalin (or other fixatives) @ 4 °C. Attach 23-gauge butterfly needle to PBS syringe.

2. Anesthetize mouse, lay mouse on its back. Open thorax, cut carefully through ribcage and diaphragm to access the heart. Work fast but do not tear any major vessels.

3. Insert the 23g butterfly needle into the left ventricle (it may be helpful to hold the needle in the left ventricle with forceps). Cut open the right ventricle for drainage, allowing the 1x PBS to be slowly but constantly perfused into the heart. If perfusion is working, liver, spleen and kidneys should turn grayish-white.

4. After most of the blood has been flushed out, unscrew PBS syringe from the butterfly and replace it with the PFA or formalin syringe. Slowly perfuse the mouse with about 20 ml of fixative. A muscle tremor will appear in the limbs and tail, and by the end of the fixative perfusion the mouse will be stiff. If perfusion is not successful at this point, the procedure should be abandoned.

5. Following perfusion, dissect out organs and tissues, transfer into labeled vials filled with fixative and store at 4 °C.

MAGNESIUM KIT
(SIGMA Diagnostics Procedure No. 595)

Reagents:

Magnesium Base Reagent (Cat. No. 595-4)
2 x 25 mL
Magnesium Color Reagent (Cat. No. 595-6)
50 mL
Magnesium Standard Solution (Cat. No. 595-2)
10 mL (2 mEq/L)

Wear lab coat, gloves, etc... Reagents are harmful(color), corrosive (base), and an irritant (standard).

Procedure:

1. Turn on Spectrophotometer. Set absorbance to 520 nm
2. Prepare Magnesium Assay Solution by mixing equal volumes of Magnesium Base Reagent and Magnesium Color Reagent. Magnesium Standard Solution is ready-to-use. Can mix all 100 mL in a bottle; store in refrigerator – Assay Solution is stable for at least 4 days.
3. Label 3 cuvettes – 1 blank and 2 standards.
4. Add 1.0 mL Assay Solution to each cuvette
5. To blank cuvette add 10 µL dH_2O
6. To each standard cuvette add 10 µL Magnesium Standard Solution
7. To each test cuvette, add 1.0 mL Assay Solution and 10 µL of your sample
8. Read and record absorbance at 520 nm of test and standards vs. blank as reference (color is stable for at least 30 minutes)
9. To determine magnesium concentration, perform the following calculations:

$$\text{Magnesium (mEq/L)} = \frac{A_{test}}{A_{standard}} \times 2.0 \text{ (Concentration of Magnesium Standard Solution)}$$

To convert to mg/dL, multiply your answer from the above equation by 1.216
To convert results into mmol/L, multiply your mg/dL answer by 0.41

Example: standard = 0.170
test = 0.140

$$\text{Magnesium (mEq/L)} = \frac{0.140}{0.170} \times 2.0 = 1.6$$

Magnesium (mg/dL) = 1.6 x 1.216 = 1.946
Magnesium (mmol/L) = 1.946 x 0.41 = .798

Background of test:

Various dye techniques have been used for magnesium determination. For this purpose, the metallochromic dye, calmagite, 1-[1-hydroxy-4-methyl-2-phenylazo]-2-naphthol-4-sulfonic acid, offers one of the best approaches. The Sigma technique is based on this reaction and proceeds as follow:

Calmagite + Magnesium ⟶ Calmagite-Magnesium Complex

The unmetallized form of the dye in the presence of magnesium forms a pink magnesium-calmagite complex that can be measured at 520 nm

INORGANIC PHOSPHORUS KIT
(SIGMA Diagnostics Procedure No. 360-UV)

Reagent:
Phosphorus Reagent (Cat. No. 360-3)
(Ammonium molybdate, 0.40 mmol/L, in sulfuric acid with surfactant)

Store Phosphorus Reagent in refrigerator (2-8°C).

Wear lab coat, gloves, etc... Reagents are harmful(color), corrosive (base), and an irritant (standard).

Procedure:
1. Turn on Spectrophotometer. Set absorbance to 340 nm
2. Label 3 cuvettes – 1 blank and 2 standards.
3. To blank cuvette add 1.0mL Phosphorus Reagent and 0.01mL of water
4. To each standard cuvette add 1.0mL Phosphorus Reagent and 0.01mL Calcium/Phosphorus Standard (Catalogue No. 360-5)
5. To each test cuvette, add 1.0 mL Phosphorus Reagent and 0.01mL of test specimen
6. Read and record absorbance of STANDARD and TEST at 340nm vs BLANK as a reference. Absorbances are stable for at least 15 minutes at room temperature.
7. To determine inorganic phosphorus concentration, perform the following calculations:

$$\text{Inorganic Phosphorus (mg/dL)} = \frac{\text{A TEST}}{\text{A STANDARD}} \times 5$$

To convert results into SI units, multiply inorganic phosphorus value (mg/dL) by 0.323.

Example: A TEST = 0.350
A STANDARD = 0.480

$$\text{Inorganic Phosphorus (mg/dL)} = \frac{0.350}{0.480} \times 5 = 3.6$$

Inorganic Phosphorus (mmol/L) = 3.6 x 0.323 = 1.16 mmol/L

Principle:

Inorganic Phosphorus + H_2SO_4 + Ammonium Molybdate

↓

Unreduced Phosphomolybdate complex

The reaction of inorganic phosphorus with ammonium molybdate in the presence of sulfuric acid (H_2SO_4), produces an unreduced phosphomolybdate complex. The absorbance of this complex at 340nm is directly proportional to the inorganic phosphorus concentration.

RAT INTACT PTH ELISA KIT
Immutopics, Inc. 96 test kit (store at 2-8°C)
Cat.# 60-2500

1. Make sure all reagents are at room temperature

2. Make sure plate washer and plate reader are available for the times when they will be needed

3. Reconstitute standards with deionized water – must sit for at least 20 minutes (with occasional gentle swirling)
→ 0 pg/ml with 2.0 ml water
→ other 5 standards and 2 controls with 1.0 ml water
→ make an extra standard between 0 and 25 (half the 25 pg/ml) since fetal PTH should give low values
→ refer to vial labels for exact concentrations!

4. Make working antibody solution (equal amounts of Rat PTH Biotinylated Antibody and Rat PTH HRP Conjugated Antibody. Mix well, stable for 7 days if stored in light-protected container at 2-8°C). ONLY make volume required for immediate use.

5. Place a sufficient number of Streptavidin Coated Strips in a holder to run PTH standards, controls and unknown samples

6. Pipet 25µl of standard, control, or sample into the designated or mapped well. **Freeze the remaining standards and controls as soon as possible after use**

7. Pipet 100µl of the Working Antibody Solution into each well

8. Cover the plate with one plate sealer, then cover with aluminum foil to avoid exposure to light

9. Incubate plate at room temperature for 3 hours on a horizontal rotor (180-220 RPM)

10. Dilute wash concentrate during this incubation period (add 190ml deionized water to 10ml wash concentrate. Store diluted wash solution at room temperature)

11. Remove the aluminum foil and plate sealer. Aspirate the contents of each well. Wash each well five times by dispensing 350µl of working wash solution into each well and then completely aspirating the contents. **Alternatively, an automated microtiter plate washer can be used** – need extra wash solution if using automated washer

12. Pipet 150µl of ELISA HRP Substrate into each of the wells

13. Re-cover the plate with the plate sealer and aluminum foil. Incubate at room temperature for 30 minutes on a horizontal rotor (180-220 RPM)
14. Remove the aluminum foil and plate sealer. Read the absorbance at 595nm within 5 minutes in a microtiter plate reader against the 0 pg/ml Standard wells as a blank

15. Immediately pipet 100µl of ELISA Stop Solution into each of the wells. Mix gently

16. Read the absorbance at 450nm within 10 minutes in the microtiter plate reader against a blank of 250µl of distilled or deionized water

Note: if wavelength correction is available, set the instrument to dual wavelength measurement at 450nm with background wavelength correction set at 595nm

- → It is recommended that all standards, controls, and samples be assayed in duplicate
- → Store light sensitive reagents (HRP Conjugated Antibody, Working Antibody Solution, and ELISA HRP Substrate) in the original amber bottles or other suitable container which is protected from the light
- → Store any unused Streptavidin Coated Strips in the resealable aluminum pouch with desiccant
- → The sample and all reagents should be pipetted carefully to prevent bubbles in wells
- → Sequence and timing of each reagent addition is important as both the immunological and enzymatic reactions are in kinetic modes. The use of an automated microtiter plate washer is strongly recommended. All pipetting and washing steps should be performed such that the timing is as consistent as possible
- → Freeze/thaw of plasma samples may accelerate clot formation. These samples must be centrifuged and decanted prior to assay to remove all particulate material which can cause random high non-specific binding on well surface

RAT CALCITONIN IRMA KIT

Immutopics, Inc.
Cat.# 50-5000

Test Principle:

The Rat Calcitonin IRMA Kit is a two-site immunoradiometric assay (IRMA) for the measurement of rat calcitonin in serum, plasma or cell culture media. Two different antibodies to rat calcitonin are used in the assay. A monoclonal antibody is immobilized onto plastic beads to capture the calcitonin molecules and an affinity purified polyclonal goat antibody is radiolabeled for detection.

A sample containing rat calcitonin is incubated simultaneously with an antibody coated bead and the ^{125}I labeled antibody. Calcitonin contained in the sample is immunologically bound by the immobilized antibody and the radiolabeled antibody to form a "sandwich" complex:

Bead/Anti-Rat Calcitonin---Rat Calcitonin---^{125}I Anti-Rat Calcitonin

At the end of the incubation period, the bead is washed to remove any unbound labeled antibody and other components. The radioactivity bound to the bead is then measured in a gamma counter. The radioactivity of the antibody complex bound to the bead is directly proportional to the amount of rat calcitonin in the sample. A standard curve is generated by plotting the CPM standard on logarithmic scales. The concentration of rat calcitonin in the samples is determined directly from this curve.

Assay Procedure:

1. Pipet 200 µL of standard, control or sample into appropriately labeled tubes
2. Pipet 100 µL of ^{125}I Labeled Rat Calcitonin Antibody into all tubes.
3. Vortex all tubes.
4. Using forceps or appropriate bead dispenser, add one bead to each tube. Tilt tube rack to approximately a 30 degree angle to prevent splashing. Cover tube rack with Parafilm or equivalent.
5. Incubate tubes at room temperature for 18 to 24 hours.
6. Aspirate the contents of each tube. Wash the beads three times by dispensing 2 mL of wash solution into each tube and then completely aspirating the contents.
7. Count each tube in a gamma counter for one minute and record the counts.

Calculation of Results:

The standard curve is generated using the rat calcitonin standards contained in the kit. Refer to individual vial labels for exact concentrations. Generate the curve as follows:

1. Calculate the average CPM for each pair of duplicate assay tubes.

2. Subtract the average CPM of the 0 pg/mL Standard from all other average CPMs to obtain corrected CPM.

3. The standard curve is generated by plotting the corrected CPM of each standard level on the ordinate against the standard concentration on the abscissa using log-log paper. Appropriate computer assisted data reduction programs may also be used for calculation of rat calcitonin results.

The rat calcitonin concentration of the controls and samples are read directly from the standard curve using their respective corrected CPM. Samples having a corrected CPM between the 0 pg/mL Standard and the next highest standard should be calculated by the formula:

$$\text{Value of unknown} = \frac{\text{Corrected CPM (unknown)}}{\text{Corrected CPM } (2^{nd}\text{ Std.})} \times \text{Value of the } 2^{nd}\text{ Std.}$$

IN SITU HYBRIDIZATION

IN SITU HYBRIDIZATION: PURIFYING LINEARIZED PLASMID

1. Increase volume to 200 µl water.
2. Add 200 µl phenol/chloroform. Vortex vigorously 10 seconds.
3. Centrifuge for 2 minutes, collect supernatant into a fresh tube.
4. Add 1/10 volume 3 M NaOAc and 2 1/2 volume EtOH.
5. Freeze on dry ice at least 5 min to precipitate DNA.
6. Centrifuge at 12,000g for 15 min in cold room.
7. Pour off supernatant.
8. Add 500 µl 70 % EtOH. Invert several times.
9. Vortex, centrifuge 10 min to ensure pellet adheres to bottom.
10. Pour off supernatant and SpeedVac until pellets are dry (approximately 20 minutes).
11. Resuspend in 10 µl water (depending on original concentration!) and store at -20°C.

IN SITU HYBRIDIZATION: LABELING RIBOPROBES

1. Linearize the plasmid containing probe of interest with appropriate restriction enzymes. Usually linearize 10 µg DNA. Check the linearization on an agarose gel, then purify by phenol/chloroform extraction and ethanol precipitation. Store at -20 °C in water at 1 µg/µl.

2. Label the probe using the SP6/T7 transcription kit (Promega).

3. Reaction mixture is:

	For ^{35}S:
5x transcription buffer	2.0 µl
100 mM DTT	1.0 µl
rATP	0.5 µl
rCTP	0.5 µl
rGTP	0.5 µl
^{35}S-UTP (125 µCi)*	3.0 µl
RNasin	0.5 µl
linearized plasmid (1 µg)	1.0 µl
appropriate polymerase	1.0 µl

*dry up to 10 µl of original solution of ^{35}S-UTP (#NEG 039H, New England Nuclear) by Speed-Vac beforehand. Dissolve the pellet with 3 µl water.

Incubate 1 hr @ 37 °C (waterbath). Then add another 1.0 µl of polymerase and incubate for an additional 1 hr @ 37 °C.

4. Add 0.5 µl RNasin
0.5 µl DNase

Incubate 15 min @ 37 °C.

5. Add

0.5 M EDTA	7 µl
5x NTE	14 µl
water	38 µl

(5x NTE= 100 mM Tris pH 7.5, 500 mM NaCl, 50 mM EDTA)

6. Remove unincorporated nucleotides with NucTrap column (Stratagene # 400702). Apply 70 µl of 1x NTE to top of resin bed and push through column. Discard the eluant. Apply sample prepared above (70 µl) and push through the column, collecting the eluant.

Apply 70 µl of 1x NTE again and push through, adding this eluant to the previous fraction.

7. Count the radioactivity of 1 µl probe in 10 ml scintillation fluid in a scintillation counter. Counts should be 0.5-1.5 x 10^6 cpm/µl.

8. Store probe at -70 °C.

9. If necessary, check the integrity of the probe by running out 5 µl of the probe on a denaturing acrylamide gel. Dry the gel and apply to film for autoradiography.

IN SITU HYBRIDIZATION: PREHYBRIDIZATION TREATMENT

All solutions are based on 600 ml volumes and dishes.

1. Put slides in slide warmer for 15 min to dry them and melt paraffin.

2. Prepare 4% paraformaldehyde (PFA) in PBS:

   540 ml water (boil before adding other ingredients!)
   600 µl 10 N NaOH
   24 g paraformaldehyde powder

Allow it to go into solution. Add 60 ml 10x PBS. Then add 600 µl diethylpyrocarbonate (DEPC) (kept in fridge). Add 200 µl 12 N HCl and check pH (it should be ~ 7.5 by filter strip check). Add more HCl or 10 N NaOH to adjust pH as needed. Then let solution cool down and pour into a dish.

3. Deparaffinize and rehydrate the sections.

a.	xylene	5 min
b.	xylene	5 min
c.	xylene	5 min
d.	100% EtOH	1 min
e.	95% EtOH	1 min
f.	70% EtOH	1 min
g.	PBS	1 min

4. 4% paraformaldehyde (PFA) in PBS for 15 min

5. PBS for 5 min

6. 10 µg/ml proteinase K in PBS @ 37 °C for 15 min
   (600 µl of 10 mg/ml proteinase K in 600 ml PBS)

7. 4% PFA in PBS for 10 min (reuse from step 4).

8. PBS for 5 min.

9. 0.2 N HCl for 10 min.
   (10 ml 12 N HCl in 600 ml water)

10. PBS for 5 min.

11. 0.1 M triethanolamine (pH 7.5) for 2 min.

(7.8 ml TEA plus 7 ml water in a 15 ml Falcon tube; vortex, then add to 600 ml water)

12. 0.25% acetic anhydride for 10 min.
(1.8 ml acetic anhydride in 5 ml water; shake vigorously in a 50 ml Falcon tube, then pour over the slides in the TEA. MAKE DIRECTLY BEFORE USE!)

13. PBS for 5 min.

14. 70% EtOH for 5 min.

15. 95% EtOH for 5 min.

16. Air-dry. Apply diluted probe to sections and apply coverslips as described.

IN SITU HYBRIDIZATION: APPLYING PROBE COCKTAIL

HYBRIDIZATION SOLUTION

final concentration	stock	for 50 ml
50% formamide	5 ml (100%)	25 ml
10 mM Tris-HCl (pH 7.6)	100 µl (1 M)	500 µl
200 µg/ml tRNA	100 µl (20 µg/µl)	500 µl
1x Denhardt's solution	200 µl (50x)	1000 µl
10% dextran sulfate	2 ml (50%)	10 ml
600 mM NaCl	1.25 ml (5 M)	6 ml
0.25% SDS (pH 8.0)	250 µl (10%)	1.25 ml
final volume	10 ml	50 ml

1. When preparing hybridization solution, dissolve dextran sulfate in water and NaCl before adding other items. Store hybridization solution @ -20 °C in 2 ml aliquots. Prior to use, add 5% v/v of 1 M dithiothreitol (DTT) to solution and add labeled probe. Always use fresh aliquots of hybridization solution and DTT.

2. Dilute probe in hybridization mixture with DTT to a final concentration of ~ 5 x 10^7 cpm/ml. Or, can usually simply use 5% probe v/v if probe count is ≥ 1 x 10^6 cpm. E.g. for 140 µl probe, use 7 µl DTT, 7 µl probe and 126 µl hybridization juice. Or use digoxigenin-labeled probe at 1% by volume and detect by alkaline phosphatase or other methods.

3. Denature diluted probe in 85 °C water bath for at least 5 min. Leave probe in water bath until ready to add to sections.

4. After prehybridization and EtOH drying of slides, apply probes to sections. Use a volume of 50-100 µl per slide, depending on the amount of tissue per slide.

5. Cover slides with parafilm coverslips, taking care to delicately press out any bubbles.

6. Incubate overnight @ 55 °C in a humidity chamber containing 50% formamide-soaked wicks.

IN SITU HYBRIDIZATION: POST HYBRIDIZATION WASHES

1. Incubate slides in 5x SSC @ 50 °C for 10 min. Prewarm the waterbath to prevent dextran from precipitating. Gently remove coverslips from the slides.

2. 2x SSC / 50% formamide @ 50 °C for 30 min.

3. TNE (10 mM Tris-HCl, pH 7.6; 500 mM NaCl; 1 mM EDTA) @ 37 °C for 10 min.

4. 10 µg/ml RNase A in TNE @ 37 °C for 30 min.
(100 µl of 20 mg/ml solution RNase A per 200 ml TNE)

5. TNE @ 37 °C for 10 min.

6. 2x SSC @ 50 °C for 20 min.

7. 0.2x SSC @ 50 °C for 20 min.

8. 0.2x SSC @ 50 °C for 20 min.

9. 70% EtOH for 5 min.

10. 70% EtOH for 5 min

11. 95% EtOH for 5 min.

12. Air-dry.

13. Autoradiography as described.

AUTORADIOGRAPHY

EQUIPMENT

Darkroom with: safelight conditions (Wratten #2)
temp 18-20 °C, rel. humidity 40-50%
water bath @ 43 °C
NTB-2 emulsion, aliquoted
2% glycerol in water
dipping jar or slide mailers for photographic emulsion
drying plate
desiccant
slide boxes (light-tight, or with aluminum foil to wrap)
Kodak developer
Kodak fixer
70% & 100% ethanol

1. Place slides in an autoradiography cassette with suitable x-ray film. Expose at room temperature overnight or longer, and develop. Use the resulting film exposure as a gauge for determining the duration of liquid emulsion exposure (roughly 4x as long to achieve the same level of signal as observed on film).

2. Aliquot the solid NTB-2 emulsion (Kodak) into eight 20 ml brown light-tight containers (Nalgene, Fisher), wrap in aluminum foil and store in a black bag at 4 °C (ideally in the darkroom). Emulsion may be stored 4 months or less.

3. Under safelight conditions, melt an aliquot of NTB-2 at 43 °C for 45-60 min. Prewarm 10 ml of 2% glycerol in water in a 15 ml tube during this time. Set up a large (1 liter) beaker with 600 ml water @ 43 °C, which will hold the dipping jar.

4. Place the dipping jar in the beaker of warm water. Pour the melted emulsion into the dipping jar, and then slowly pour in the prewarmed 2% glycerol in water (avoid causing bubbles). Dip a clean slide in and out several times to mix the emulsion with the 2% glycerol in water. Check that emulsion is bubble-free by examining the slide for an even coating. Repeat this until the bubbles are removed, if needed.

5. Next dip the experimental slides, allowing each to drain vertically for 2 sec., and blot the end on paper. Immediately place the slide inverted (marking side down) on a slide rack to dry.

6. When the last of the slides are dipped, transfer slides to slide boxes containing a sachet of desiccant. Be careful to place the boxes on edge so that the slides will remain inverted.

7. Wrap each slide box with three sheets of aluminum foil, seal with tape, and place at 4 °C. If possible, place at room temperature overnight to avoid rapid cooling, then move to 4 °C.

8. After a suitable interval of exposure time (determined in step 1 above) remove the box of slides from the cold room and warm to room temperature (>1 hr.)

9. Under safelight conditions in a darkroom, transfer the slides into a slide rack and pass through the following:

a.	Kodak DEKTOL developer	2 min
	(dissolve 17 g per 250 ml water)	
b.	distilled water	15 sec
c.	Kodak fixer	5 min
	(dissolve 45 g per 250 ml water)	
d.	distilled water	5 min
e.	dry in dust-free atmosphere	

Prepare fresh developer each day. Use at least 5 ml of each reagent per slide.

10. Turn lights on.

11. Air-dry.

12. Proceed with Hematoxylin and eosin staining.

hematoxylin	90 sec
water	2 min or longer (scrape emulsion off back of slide)
eosin	3 min
70% EtOH	1 min
80% EtOH	1 min
90% EtOH	1 min
100% EtOH	1 min
100% EtOH	1 min
xylene	1 min
xylene	1 min
xylene	1 min

13. Apply mounting media and glass coverslip. Set aside to dry.